Multiple quantum exceptional, diabolical, and hybrid points in multimode bosonic systems: I. Inherited and genuine singularities

Kishore Thapliyal[1], Jan Peřina Jr.[1], Grzegorz Chimczak[2],
Anna Kowalewska-Kudłaszyk[2], and Adam Miranowicz[2]

[1]Joint Laboratory of Optics, Faculty of Science, Palacký University, Czech Republic, 17. listopadu 12, 771 46 Olomouc, Czech Republic

[2]Institute of Spintronics and Quantum Information, Faculty of Physics, Adam Mickiewicz University, 61-614 Poznań, Poland

The existence and degeneracies of quantum exceptional, diabolical, and hybrid (i.e., diabolically degenerated exceptional) singularities of simple bosonic systems composed of up to five modes with damping and/or amplification are analyzed. Their dynamics governed by quadratic non-Hermitian Hamiltonians is followed using the Heisenberg-Langevin equations. Their dynamical matrices generally exhibit specific structures that allow for an effective reduction of their dimension by half. This facilitates analytical treatment and enables efficient spectral analysis based on characteristic second-order diabolical degeneracies. Conditions for the observation of inherited quantum hybrid points, observed directly in the dynamics of field operators, having up to third-order exceptional and second-order diabolical degeneracies are revealed. Surprisingly, exceptional degeneracies of only second and third orders are revealed, even though the systems with up to five modes are considered. Exceptional and diabolical genuine points and their degeneracies observed in the dynamics of second-order field-operator moments are also analyzed. Each analyzed bosonic system exhibits its own unique and complex dynamical behavior.

1 Introduction

Non-Hermitian Hamiltonians had been for a long time considered not being suitable for describing real physical systems. This opinion has changed after the seminal work by Bender and Boettcher [1] who showed that the non-Hermitian Hamiltonians endowed with a parity and time symmetry ($\mathcal{PT}$-symmetry) exhibit real spectra in certain areas of the system parameter space. This leads to the formulation of new area of physics, i.e., non-Hermitian quantum mechanics [2–5], which has already provided numerous models [6–11] suitable for describing real quantum systems in many areas of physics. Moreover, non-Hermitian Hamiltonians exhibit new algebraic structures: It has been shown that, for certain values of parameters, there occur spectral degeneracies accompanied by degeneracies of the eigenvectors of a given Hamiltonian. Such points in a system parameter

space with exceptional degeneracies (EDs) are called exceptional points (EPs) for which the dimension of the corresponding Hilbert space is reduced. This has interesting physical consequences and leads to new unexpected physical effects. It allows to enhance the precision of measurements of suitable physical quantities [12–16]. It also leads to enhanced nonlinear interactions [17, 18]. For this reason, $\mathcal{PT}$-symmetric systems of different kinds have been found appealing in many areas of physics including: optical waveguides [19, 20], optical lattices [21–24], spin lasers [25], optical coupled structures [26–30], coupled optical microresonators [13, 31–35], quantum-electrodynamics circuits (QED) [36], systems with complex potentials [37], optomechanical systems [38, 39], photonics molecules [40], among others. Moreover, schemes for engineering properties of EPs have been suggested (see, e.g., [41] and references therein).

Subsequent studies have revealed also other features observed in $\mathcal{PT}$-symmetric systems in addition to EPs. For example, the spectral degeneracies which are not accompanied by the corresponding eigenvector degeneracies, were observed [42]. Such degeneracies do not usually lead to the above discussed physical effects and so the corresponding points in the system parameter space were named diabolical points (DPs). Note that DPs, contrary to EPs, can also be observed in Hermitian systems [42]. As pointed out in [43], it may happen that this DP with its diabolical degeneracy (DD) occurs at an EP. In this case, 'independent' (i.e. with different eigenvectors) multiple spectral and eigenvector degeneracies are found in systems and we refer to them as hybrid diabolic exceptional points (HPs). Such systems then naturally exhibit a physical behavior similar to that observed at EPs. Moreover, new effects originating in diabolical degeneracy may arise. For example, the system behavior when encircling an HP has been used to construct a multi-mode optical switch [44].

Non-Hermitian $\mathcal{PT}$-symmetric optical bosonic systems are especially interesting from the point of view of their behavior at EPs. Their infinite-dimensional Hilbert space leads to numerous manifestations of modifications of their dynamics at quantum EPs (QEPs), i.e. EPs observed in quantum systems [18], including the effect of quantum jumps [45, 46]. The system dynamics may be followed either directly in the Hilbert space [the Liouville space of statistical operators] or in the complementary space of field-operator moments (FOMs) of all orders [47, 48]. The studies performed in the moment space of field operators in multimode bosonic systems described by non-Hermitian quadratic Hamiltonians revealed different types of degeneracies related to QEPs [43, 49]. Moreover, they allowed to sort QEPs into three classes: inherited QEPs, genuine QEPs and induced QEPs. The dynamical equations for the mean values of field operators indicated the presence of inherited QEPs and quantum HPs (QHPs) [43] that represent the core of the studied unusual behavior. The presence of such inherited QEPs and QHPs then implies the existence of genuine QEPs and QHPs [43] observed in the dynamics of higher-order FOMs. With the increasing FOM order, the degeneracies of genuine QEPs and QHPs increase. Moreover, similar or identical FOMs, as being related by the field commutation relations, arise in the formal construction of higher-order FOMs. Thus, we can also define induced QEPs and QHPs [43] that further enlarge the multiplicity of the spectral degeneracies. However, as these redundant FOMs share their time evolution with the FOMs contributing to genuine QEPs and QHPs, they do not lead to additional diversity of the system evolution. Thus, they are not interesting from the point of view of the dynamics of FOMs of a given order. This dynamics is fully characterized by the corresponding genuine QEPs and QHPs. As the properties of genuine QEPs and QHPs originate in those of the inherited QEPs and QHPs, the analysis of the latter is crucial for the understanding of a system evolution. For this reason, it is important to identify the inherited QEPs and QHPs and their de-

generacies in simple bosonic systems formed by smaller numbers of bosonic modes. This analysis may then be exploited for further studies of physical effects in such systems.

The system composed of two mutually interacting modes, one being damped and the other amplified, was already analyzed from this point of view in Ref. [43]. This analysis may be considered as the simplest building block useful for investigations of more complex bosonic systems in which much richer and diverse physical behavior is expected. Here, we consider systems composed of up to five modes in different configurations promising for the observation of QEPs and QHPs. Looking for inherited QEPs with higher-order EDs is the main goal of our investigations. It is motivated by the fact that the higher is the ED order, the more modified is the system dynamics at a QEP. This then enhances the physical effects specific to QEPs like improvement in measurement precision or enhancement of nonlinear effects.

As, surprisingly, we have been able to reveal only up to the third-order ED of QEPs in the analyzed systems, we continue our analysis in Ref. [50], being the second part of this paper, in which we pay attention to the spectral degeneracies of non-Hermitian Hamiltonians observed only in specific subspaces of the systems' Liouville spaces as well as non-Hermitian Hamiltonians with unidirectional coupling. In particular, systems with unidirectional coupling exhibit significantly stronger non-Hermitian features compared to those analyzed here, enabling the observation of QEPs and QHPs of arbitrary order. In Ref. [50], we also address numerical identification of QEPs and QHPs, useful in the bosonic systems with higher dimensions. We also extend the analysis of the genuine and induced QEPs and QHPs by considering the FOMs of a general order.

At the end of Introduction, we would like to note that while the existence of higher-order EPs has been discussed previously in the literature, those analyses typically rely on semiclassical models that neglect quantum fluctuations, that are necessary for quantum consistency of the models. Moreover, many prior works investigate the spectra of semiclassical non-Hermitian Hamiltonians, which exhibit infinite (though countable) sets of eigenfrequencies. In contrast, the physically relevant spectra are those of the corresponding dynamical matrices governing the evolution equations (e.g., the Heisenberg ones in the Heisenberg picture), which involve only a small number of frequencies. It is precisely these frequencies that determine the observable behavior of the system. In semiclassical models, higher-order EPs can often be identified with relative ease. However, the validity of such models is generally restricted to specific conditions, such as short evolution times or weak damping/amplification. This raises a critical and largely unexplored question: What are the spectral degeneracies in PT-symmetric bosonic systems under general conditions, where fluctuating quantum forces - governed by fluctuation-dissipation theorems - play a non-negligible role?

The paper is organized as follows. A two-mode bosonic system with unequal damping and/or amplification rates, as the simplest considered model, is analyzed in Sec. II. Section III brings the analysis of a related three-mode system in the linear configuration. The corresponding generalized four-mode systems in their linear and circular configurations are investigated in Sec. IV whereas the analysis of the five-mode systems in their linear and pyramid configurations is found in Sec. V. Section VI brings conclusions. In Appendix A, the eigenvalues and eigenvectors of the general $2n \times 2n$ dynamical matrices are summarized. The structure of the second-order FOMs for the analyzed systems is detailed in the tables provided in Appendix B.

2 Two-mode bosonic system: Basic building blocks

We begin with the consideration of one of the simplest $\mathcal{PT}$-symmetric bosonic systems that is composed of two modes: one being attenuated and the other amplified [for the scheme, see Fig. 1(a)]. We note that even a one-mode bosonic system may exhibit $\mathcal{PT}$-symmetric behavior, as shown in Ref. [51]. We also pay attention only to the systems described by quadratic Hamiltonians that lead to linear exactly-solvable Heisenberg equations. Though these Hamiltonians lead to linear dynamical equations, they allow for describing the non-linear effect of photon-pair generation and annihilation. This effect is commonly used in various quantum optical systems to generate entangled [52] and squeezed [53, 54] states of light. $\mathcal{PT}$-symmetry restricts the form of the studied non-Hermitian Hamiltonian such that the underlying dynamics is described by the dynamical matrix composed of characteristic 2×2 submatrices. They are also used to build the matrices of more complex $\mathcal{PT}$-symmetric bosonic systems. The characteristic block structure — typical of bosonic systems with quadratic Hamiltonians — forms a critical ingredient of the analytical framework presented below, allowing us to uncover the complex structures of eigenvalues and their associated eigenvectors of the corresponding dynamical matrices in the space of system's parameters. Moreover, we also consider bosonic systems in which damping and amplification are not in balance, which is a typical situation of $\mathcal{PT}$-symmetric systems. In this unbalanced case, relying on the results presented in Ref. [55], we may introduce a specific interaction picture in which the average damping or amplification dynamics is projected out and the remaining dynamics exhibits the features found in $\mathcal{PT}$-symmetric systems.

Under these conditions, we may write the quadratic Hamiltonian of the considered two-mode bosonic system in the interaction picture as follows:

$$\hat{H}_2 = \left[\hbar \epsilon \hat{a}_1^\dagger \hat{a}_2 + \hbar \kappa \hat{a}_1 \hat{a}_2 \right] + \text{H.c.}, \tag{1}$$

where $\hat{a}_j$ ($\hat{a}_j^\dagger$) stands for the annihilation (creation) operator of the jth mode, $j = 1, 2$, ϵ is the linear coupling strength between the modes, and κ is the nonlinear coupling strength between the modes. Symbol H.c. replaces the Hermitian-conjugated terms. Whereas the linear coupling originates in the spatial overlap of the mode electric-field amplitudes, the nonlinear coupling arises in the three-mode parametric process with strong pumping [56]. The damping (amplification) of modes occurs as a consequence of the interaction with the reservoir whose two-level atoms are in the ground (excited) state [43]. Projecting out the reservoir two-level atoms, we are left with the damping (amplification) rate γ_j of jth damped (amplified) mode and the corresponding Langevin stochastic operator forces, $\hat{L}_j$ and $\hat{L}_j^\dagger$, in the dynamical Heisenberg-Langevin equations. We note that properties of the Langevin operator forces differ for the damping and amplification processes and they have to be chosen such that the field-operator commutation relations are fulfilled. This results in the corresponding fluctuation-dissipation theorems [47, 57] formulated within the Heisenberg-Langevin formalism.

Using the two-mode Hamiltonian in Eq. (1), we derive the Heisenberg-Langevin equations written for the vector $\hat{\boldsymbol{a}} = [\hat{\boldsymbol{a_1}}, \hat{\boldsymbol{a_2}}]^T \equiv \left[\hat{a}_1, \hat{a}_1^\dagger, \hat{a}_2, \hat{a}_2^\dagger \right]^T$ of field operators and vector $\hat{\boldsymbol{L}} = \left[\hat{L}_1, \hat{L}_1^\dagger, \hat{L}_2, \hat{L}_2^\dagger \right]^T$ of the Langevin operator forces as follows [58]:

$$\frac{d\hat{\boldsymbol{a}}}{dt} = -i\boldsymbol{M^{(2)}}\hat{\boldsymbol{a}} + \hat{\boldsymbol{L}}. \tag{2}$$
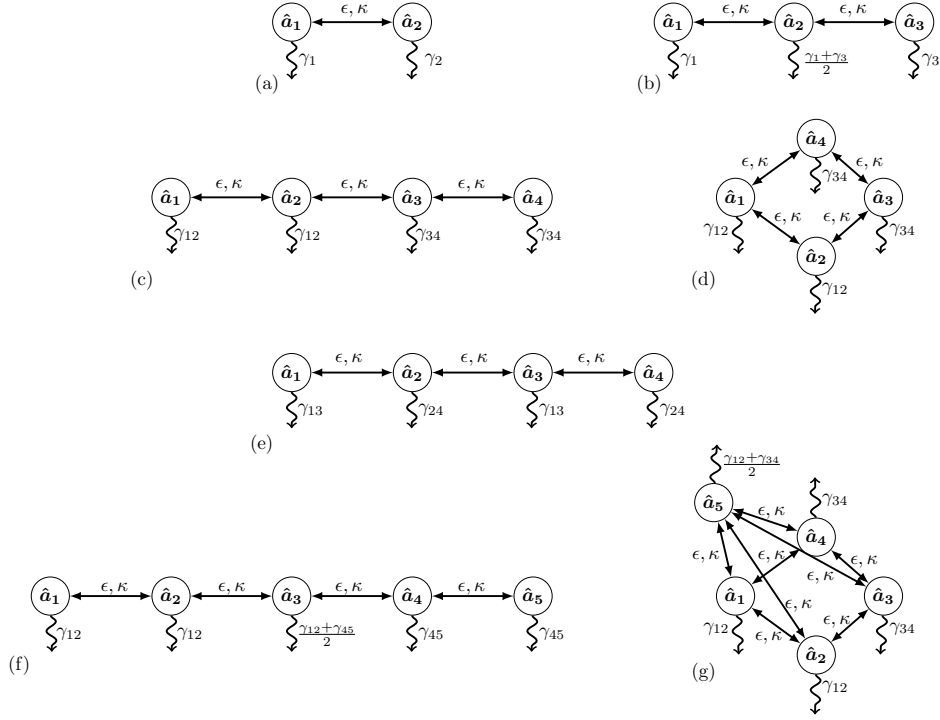
Figure 1: Schematic diagrams of the bosonic systems composed of (a) two, (b) three, (c—e) four, and (f,g) five modes with typical linear, circular, and pyramid configurations that exhibit quantum exceptional points (QEPs) and quantum hybrid points (QHPs) with various exceptional degeneracies (EDs) and diabolical degeneracies (DDs) observed in the dynamics of field-operator moments (FOMs) of different orders. Strengths ϵ and κ characterize, respectively, the linear and nonlinear coupling between the modes, γ, with subscripts indicating the mode number(s), are the damping or amplification rates, and annihilation operators $\hat{a}$ identify the mode number via their subscripts, and γ_{jk} indicates that $\gamma_j = \gamma_k$.

In Eq. (2), the dynamical matrix $M^{(2)}$,

$$M^{(2)} = \begin{bmatrix} -i\tilde{\gamma}_1 & \xi \\ \xi & -i\tilde{\gamma}_2 \end{bmatrix}, \tag{3}$$

is expressed in terms of 2×2 submatrices $\tilde{\gamma}_j$, $j = 1, 2$, and ξ is defined as:

$$\tilde{\gamma}_j = \begin{bmatrix} \gamma_j/2 & 0 \\ 0 & \gamma_j/2 \end{bmatrix}, \quad \xi = \begin{bmatrix} \epsilon & \kappa \\ -\kappa & -\epsilon \end{bmatrix}, \tag{4}$$

where γ_j is the damping or amplification rate of the mode j that is accompanied by the corresponding Langevin operator forces.

The 2×2 matrices, $\tilde{\gamma}_j$ ($j = 1, 2$) and ξ, given in Eq. (4) can be simultaneously diagonalized using the diagonalization transformation appropriate to the matrix ξ as the remaining two matrices are linearly proportional to the unity matrix and, thus, are not modified by the transformation. This diagonalization transformation then decomposes the 4×4 matrix $M^{(2)}$ in Eq. (3) into the direct sum of two independent 2×2 matrices belonging to the eigenvalues λ_1^ξ and λ_2^ξ of the matrix ξ [see Eq. (7) below] and having the

structure of the original 2×2 matrix $\boldsymbol{M^{(2)}}$:

$$\boldsymbol{M^{(2)}} = \begin{bmatrix} -i\gamma_1/2 & 0 & \lambda_1^\xi & 0 \\ 0 & -i\gamma_1/2 & 0 & \lambda_2^\xi \\ \lambda_1^\xi & 0 & -i\gamma_2/2 & 0 \\ 0 & \lambda_2^\xi & 0 & -i\gamma_2/2 \end{bmatrix}.$$

This step is critical to our analytical approach, and it is applied analogously to systems with a larger number of bosonic modes. It enables an effective reduction in the dimensionality of the diagonalization problem, thereby allowing the derivation of comprehensive analytical expressions essential for analyzing QEPs and QDPs. Denoting a general eigenvalue of the 2×2 matrix $\boldsymbol{\xi}$ as ξ, we may express the eigenfrequencies $\lambda_{1,2}^{M^{(2)}}$ and eigenvectors $\boldsymbol{y_{1,2}^{M^{(2)}}}$ of the decomposing 2×2 matrices of the 4×4 matrix $\boldsymbol{M^{(2)}}$ in Eq. (2) in the following common form:

$$\lambda_{1,2}^{M^{(2)}} = -i\gamma_+ \mp \beta \tag{5}$$

and

$$\boldsymbol{y_{1,2}^{M^{(2)}}} = \left[-\frac{i\gamma_- \pm \beta}{\xi}, 1 \right]^T, \tag{6}$$

where $4\gamma_\pm = \gamma_1 \pm \gamma_2$ and $\beta^2 = \xi^2 - \gamma_-^2$.

The eigenvalues $\lambda_{1,2}^\xi$ and the corresponding eigenvectors $\boldsymbol{y_{1,2}^\xi}$ of the matrix $\boldsymbol{\xi}$ are simply derived in the form:

$$\lambda_{1,2}^\xi = \mp\zeta \tag{7}$$

and

$$\boldsymbol{y_{1,2}^\xi} = \left[-\frac{\epsilon \mp \zeta}{\kappa}, 1 \right]^T, \tag{8}$$

where $\zeta = \sqrt{\epsilon^2 - \kappa^2}$.

Combing the above two results for the matrix diagonalization, we can express the eigenvalues $\Lambda^{M^{(2)}}$ of the 4×4 matrix $\boldsymbol{M^{(2)}}$ in Eq. (2) as $\Lambda_{1,3}^{M^{(2)}} = \lambda_{1,2}^{M^{(2)}}$ for $\xi = \lambda_1^\xi$ and $\Lambda_{2,4}^{M^{(2)}} = \lambda_{1,2}^{M^{(2)}}$ for $\xi = \lambda_2^\xi$, i.e.:

$$\begin{aligned} \Lambda_1^{M^{(2)}} &= \Lambda_2^{M^{(2)}} = -i\gamma_+ - \beta, \\ \Lambda_3^{M^{(2)}} &= \Lambda_4^{M^{(2)}} = -i\gamma_+ + \beta, \end{aligned} \tag{9}$$

and $\beta = \sqrt{\zeta^2 - \gamma_-^2}$. We note that, in general, we use capital Greek letters Λ to denote the eigenvalues of the dynamical matrices $\boldsymbol{M}$ in their full dimensions, and lowercase Greek letters λ for the eigenvalues in the reduced (half) dimensions. We also note that the average damping or amplification rate $\gamma_+ = 0$ in the usual $\mathcal{PT}$-symmetric systems, that are, however, only specific cases in our general calculations.

Similarly as the eigenvalues, we obtain the eigenvectors along the formulas

$$\begin{aligned} \boldsymbol{Y_j^{M^{(2)}}} &= \left[y_{1,1}^{M^{(2)}}(\xi = \lambda_j^\xi)\boldsymbol{y_j^\xi}, y_{1,2}^{M^{(2)}}(\xi = \lambda_j^\xi)\boldsymbol{y_j^\xi} \right]^T, \\ &\quad \text{for } j = 1, 2, \\ \boldsymbol{Y_j^{M^{(2)}}} &= \left[y_{2,1}^{M^{(2)}}(\xi = \lambda_{j-2}^\xi)\boldsymbol{y_{j-2}^\xi}, y_{2,2}^{M^{(2)}}(\xi = \lambda_{j-2}^\xi)\boldsymbol{y_{j-2}^\xi} \right]^T, \\ &\quad \text{for } j = 3, 4, \end{aligned} \tag{10}$$

$$\Lambda_{2j-1}^{M^{(n)}} = \lambda_j^{M^{(n)}}(\xi = \lambda_1^{\xi}) \qquad\qquad \Lambda_{2j}^{M^{(n)}} = \lambda_j^{M^{(n)}}(\xi = \lambda_2^{\xi})$$

$$\boldsymbol{Y_{2j-1}^{M^{(n)}}} = \begin{bmatrix} y_{j,1}^{M^{(n)}}(\xi = \lambda_1^{\xi})\begin{bmatrix} y_{1,1}^{\xi} \\ y_{1,2}^{\xi} \end{bmatrix} \\ y_{j,2}^{M^{(n)}}(\xi = \lambda_1^{\xi})\begin{bmatrix} y_{1,1}^{\xi} \\ y_{1,2}^{\xi} \end{bmatrix} \\ \cdots \\ y_{j,n}^{M^{(n)}}(\xi = \lambda_1^{\xi})\begin{bmatrix} y_{1,1}^{\xi} \\ y_{1,2}^{\xi} \end{bmatrix} \end{bmatrix} \qquad \boldsymbol{Y_{2j}^{M^{(n)}}} = \begin{bmatrix} y_{j,1}^{M^{(n)}}(\xi = \lambda_2^{\xi})\begin{bmatrix} y_{2,1}^{\xi} \\ y_{2,2}^{\xi} \end{bmatrix} \\ y_{j,2}^{M^{(n)}}(\xi = \lambda_2^{\xi})\begin{bmatrix} y_{2,1}^{\xi} \\ y_{2,2}^{\xi} \end{bmatrix} \\ \cdots \\ y_{j,n}^{M^{(n)}}(\xi = \lambda_2^{\xi})\begin{bmatrix} y_{2,1}^{\xi} \\ y_{2,2}^{\xi} \end{bmatrix} \end{bmatrix}$$

$$j = 1, \ldots, n.$$

Figure 2: Schematic diagram of the structure of eigenvalues $\Lambda_j^{M^{(n)}}$ and the corresponding eigenvectors $\boldsymbol{Y_j^{M^{(n)}}}$, $j = 1, \ldots, 2n$, of a general dynamical $2n \times 2n$ matrix $\boldsymbol{M^{(n)}}$ built from the eigenvalues $\lambda_k^{M^{(n)}}$ and the corresponding eigenvectors $\boldsymbol{y_k^{M^{(n)}}}$, $k = 1, \ldots, n$, of the matrix $\boldsymbol{M^{(n)}}$ considered as an $n \times n$ matrix composed of 2×2 submatrices at the positions of its elements; $n = 2, 3, \ldots$. The eigenvalues $\lambda_{1,2}^{\xi}$ and the corresponding eigenvectors $\boldsymbol{y_{1,2}^{\xi}}$ belong to the submatrix $\boldsymbol{\xi}$.

in the form:

$$\begin{aligned} \boldsymbol{Y_{1,2}^{M^{(2)}}} &= \left[\ \frac{(\mp\epsilon+\zeta)\chi}{\kappa\zeta}, \quad \pm\frac{\chi}{\zeta}, \quad -\frac{(\epsilon\mp\zeta)}{\kappa}, \quad 1\ \right]^T, \\ \boldsymbol{Y_{3,4}^{M^{(2)}}} &= \left[\ \frac{(\pm\epsilon-\zeta)\chi^*}{\kappa\zeta}, \quad \mp\frac{\chi^*}{\zeta}, \quad -\frac{(\epsilon\mp\zeta)}{\kappa}, \quad 1\ \right]^T, \end{aligned} \tag{11}$$

where $\chi = i\gamma_- + \beta$. The structure of eigenvalues and eigenvectors of a general dynamical $2n \times 2n$ matrix $\boldsymbol{M^{(n)}}$ formed by the eigenvalues $\lambda_k^{M^{(n)}}$ and eigenvectors $\boldsymbol{y_k^{M^{(n)}}}$ of the $n \times n$ matrix $\boldsymbol{M^{(n)}}$ expressed using 2×2 submatrices and the eigenvalues $\lambda_{1,2}^{\xi}$ and eigenvectors of the submatrix $\boldsymbol{\xi}$ is shown in Fig. 2.

The formula in Eq. (9) provides the two pairs of coinciding eigenvalues. However, Eq. (11) for the corresponding eigenvectors reveal no eigenvector degeneracy in general. On the other hand, χ is purely imaginary for $\beta = 0$, which leads to $\boldsymbol{Y_1^{M^{(2)}}} = \boldsymbol{Y_3^{M^{(2)}}}$ and $\boldsymbol{Y_2^{M^{(2)}}} = \boldsymbol{Y_4^{M^{(2)}}}$, while having all the eigenvalues the same. So we observe the second-order degeneration in the Hilbert space that is formed by two second-order QEPs with identical eigenvalues. We, thus, have a QHP with second-order DD and ED in this case. The condition $\beta = 0$ implies that the eigenvalues and eigenvectors of the 2×2 matrix $\boldsymbol{M^{(2)}}$ given in Eqs. (5) and (6) coincide. The second-order ED, thus, originates in the 2×2 form of matrix $\boldsymbol{M^{(2)}}$. We note that this degeneracy can be verified by transforming the matrix $\boldsymbol{M^{(2)}}$ for $\beta = 0$ into its Jordan form

$$\boldsymbol{J_{M^{(2)}}} = \begin{bmatrix} -i\gamma_+ & 1 \\ 0 & -i\gamma_+ \end{bmatrix}. \tag{12}$$

On the other hand, the eigenvalues of 2×2 submatrix $\boldsymbol{\xi}$ written in Eq. (7) point out at the origin of DD: They differ just by the sign, but they lead to the same value of β, i.e., to the same eigenvalue $\lambda_{1,2}^{M^{(2)}}$ of the 2×2 matrix $\boldsymbol{M^{(2)}}$. DD is then implied by the fact that the eigenvectors $\boldsymbol{y_{1,2}^{\xi}}$ of 2×2 submatrix $\boldsymbol{\xi}$ in Eq. (8) differ for $\zeta \neq 0$.

These findings about the structure of the matrices describing the dynamical equations have their counterpart in the structure of the analyzed two-mode $\mathcal{PT}$-symmetric system. The 2×2 matrix $\boldsymbol{\xi}$, defined in Eq. (4), connects pairs of the annihilation and creation operators of different modes. As such it forms the basic building block of more complex $\mathcal{PT}$-symmetric systems, together with the damping and/or amplification matrices $\tilde{\boldsymbol{\gamma}}_j$ in Eq. (4). In more complex $\mathcal{PT}$-symmetric systems, the dependencies of the eigenvalues of the dynamical $n \times n$ matrices $\boldsymbol{M^{(n)}}$ ($n = 2, 3, \ldots$) on the eigenvalues $\lambda_{1,2}^{\xi}$ of the $\boldsymbol{\xi}$

matrix are typically quadratic. This, thus, results in the observation of second-order DD in the dynamical features of the matrices $\boldsymbol{M^{(n)}}$. In this case, the eigenvalue analysis of the considered systems considerably simplifies and we may restrict our attention to only the $n \times n$ matrices $\boldsymbol{M^{(n)}}$ with their elements in the form of 2×2 submatrices, when a detailed eigenvalue analysis is performed. The consequences of the eigenvalue analysis are then combined with the above second-order DD.

The condition $\beta = 0$ for observing QHPs can be analyzed in the space of system parameters $(\epsilon, \kappa, \gamma_1, \gamma_2)$ as follows. The quadratic Hamiltonian $\hat{H}^{(2)}$ in Eq. (1) provides the linear Heisenberg-Langevin equations that allow for the temporal rescaling ϵt, i.e., only the relative parameters $(\kappa/\epsilon, \gamma_1/\epsilon, \gamma_2/\epsilon)$ suffice in characterizing the system dynamics. Moreover, the structure of the analyzed systems is such that the average damping or amplification rate γ_+ influences equally only the eigenvalues, but it does not modify the eigenvectors. This makes the space of the system parameters effectively two-dimensional with the spanning parameters $(\kappa/\epsilon, \gamma_-/\epsilon)$. Using these parameters, the condition $\beta = 0$ is expressed as follows:

$$\frac{\kappa^2}{\epsilon^2} + \frac{\gamma_-^2}{\epsilon^2} = 1. \tag{13}$$

Thus, the QHPs form a circle with the unit radius in the space $(\kappa/\epsilon, \gamma_-/\epsilon)$, as shown by the red dashed curve in Fig. 3(a). We note that, at this circle, there is a specific point at $\gamma_- = 0$ in which all four eigenvectors, given in Eq. (10), are the same which gives raise to the fourth-order QEP. However, this corresponds to the system in which both modes are equally damped or amplified. It is worth noting that the eigenvectors of both matrices $\boldsymbol{M^{(2)}}$, given in Eq. (3), and $\boldsymbol{\xi}$, in Eq. (4), are degenerated at this point.

Deeper insight into the structure of higher-order FOMs, as well as the system dynamics, can be obtained once we transform the Heisenberg-Langevin equations (2) into the form in which the dynamical matrix has the diagonal form. Using the transformation matrix $\boldsymbol{P} = \left[\boldsymbol{Y_1^{M^{(2)}}}, \boldsymbol{Y_2^{M^{(2)}}}, \boldsymbol{Y_3^{M^{(2)}}}, \boldsymbol{Y_4^{M^{(2)}}} \right]$ formed from the eigenvectors in Eq. (10), we define the corresponding field operators $\hat{\boldsymbol{b}} = \left[\hat{b}_1, \hat{b}_2, \hat{b}_1^\dagger, \hat{b}_2^\dagger \right]^T$, the Langevin operator forces $\hat{\boldsymbol{K}} = \left[\hat{K}_1, \hat{K}_2, \hat{K}_1^\dagger, \hat{K}_2^\dagger \right]^T$, and the diagonal dynamical matrix $\boldsymbol{\Lambda^{(2)}}$:

$$\boldsymbol{\Lambda^{(2)}} = \boldsymbol{P}^{-1} \boldsymbol{M^{(2)}} \boldsymbol{P}, \quad \hat{\boldsymbol{b}} = \boldsymbol{P}^{-1} \hat{\boldsymbol{a}}, \quad \hat{\boldsymbol{K}} = \boldsymbol{P}^{-1} \hat{\boldsymbol{L}}. \tag{14}$$

We note that the order of elements in the operator vector $\hat{\boldsymbol{b}}$ (and similarly in the vector $\hat{\boldsymbol{K}}$ of the accompanying Langevin operator forces) is given by the numbering of the eigenvalues in Eq. (9) and the corresponding diagonalization transform.

In the transformed basis, the Heisenberg-Langevin equations take the form:

$$\frac{d\hat{\boldsymbol{b}}}{dt} = -i\boldsymbol{\Lambda^{(2)}}\hat{\boldsymbol{b}} + \hat{\boldsymbol{K}}. \tag{15}$$

We note that the positions of the newly-defined annihilation and creation operators in the vector $\hat{\boldsymbol{b}}$, as well as the positions of the accompanying Langevin operator forces in the vector $\hat{\boldsymbol{K}}$, differ from those in the original vectors $\hat{\boldsymbol{a}}$ and $\hat{\boldsymbol{L}}$ defined above Eq. (2). The solution to Eq. (15) is expressed as:

$$\begin{aligned} \hat{\boldsymbol{b}}(t) &= \exp(-i\boldsymbol{\Lambda^{(2)}}t)\hat{\boldsymbol{b}}(0) \\ &\quad + \int_0^t dt' \exp[-i\boldsymbol{\Lambda^{(2)}}(t-t')]\hat{\boldsymbol{K}}(t'). \end{aligned} \tag{16}$$
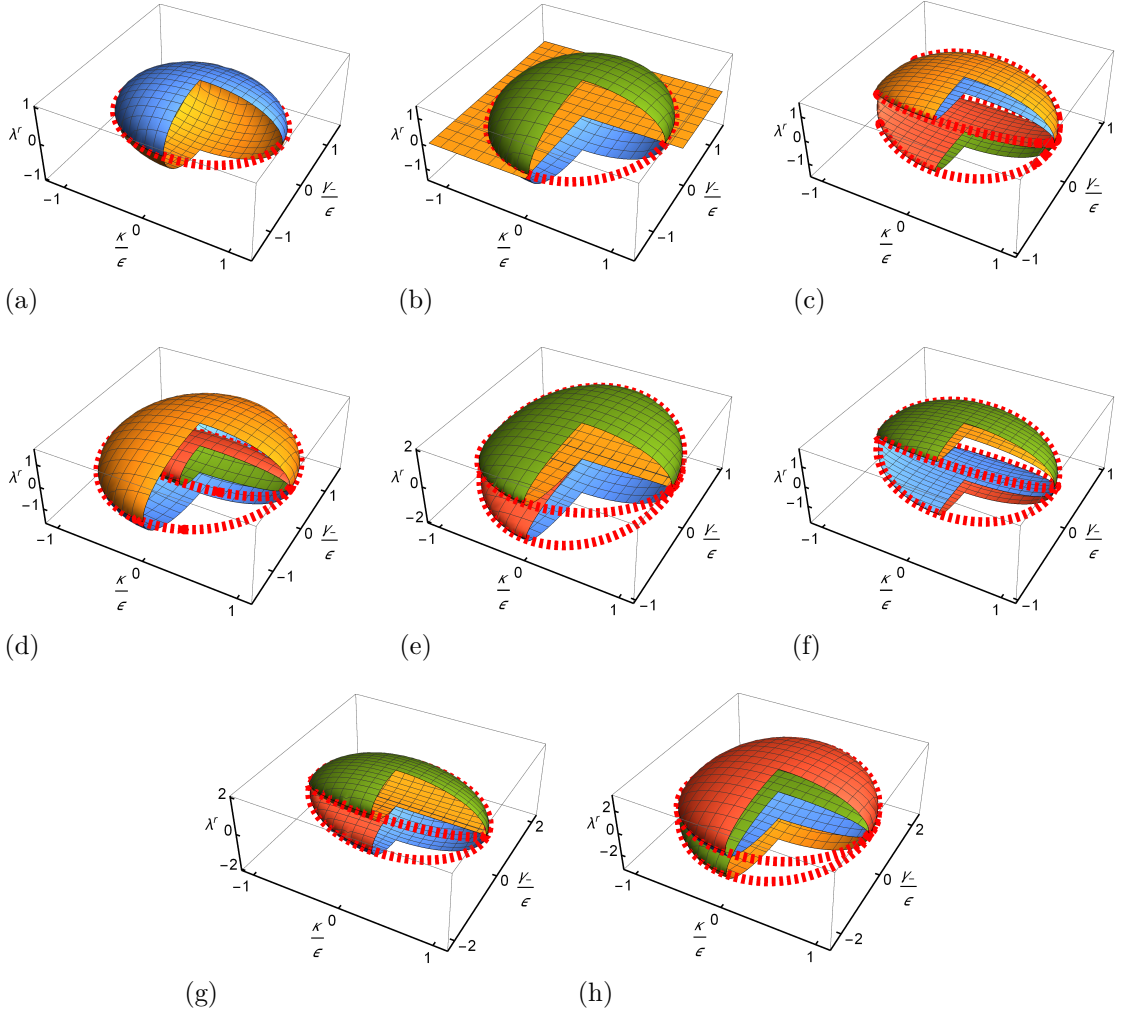
Figure 3: Real parts λ^{r} of the eigenvalues (a) $\lambda_{1,2}^{M^{(2)}}$ of the matrix $\boldsymbol{M^{(2)}}$, given in Eq. (5), for the two-mode bosonic system, (b) $\lambda_{1,2,3}^{M^{(3)}}$ of the matrix $\boldsymbol{M^{(3)}}$, given in Eq. (23), for the three-mode linear bosonic system, (c) [(d)] $\lambda_{1,\dots,4}^{M_{l1}^{(4)}}$ $[\lambda_{1,\dots,4}^{M_{l2}^{(4)}}]$ of the matrix $\boldsymbol{M_{l1}^{(4)}}$ $[\boldsymbol{M_{l2}^{(4)}}]$, given in Eq. (30) [(34)] for the four-mode linear bosonic system with neighbor modes having equal [different] damping and/or amplification rates, (e) $\lambda_{1,\dots,4}^{M_{c1}^{(4)}}$ of the matrix $\boldsymbol{M_{c1}^{(4)}}$, given in Eq. (40), for the four-mode circular bosonic system with neighbor modes having equal damping and/or amplification rates, (f) $\lambda_{2,\dots,5}^{M_{l}^{(5)}}$ of the matrix $\boldsymbol{M_{l}^{(5)}}$, given by Eq. (47), for the five-mode linear bosonic system, and (g,h) $\lambda_{2,\dots,5}^{M_{P}^{(5)}}$ of the matrix $\boldsymbol{M_{P}^{(5)}}$, given in Eq. (54), for the five-mode pyramid bosonic system assuming (g) $\beta_1 = 0$ and (h) $\beta_2 = 0$. The eigenvalues are drawn in the parameter space $(\kappa/\epsilon, \gamma_-/\epsilon)$, where ϵ (κ) is the linear (nonlinear) coupling strength and γ_- the difference of the damping/amplification rates in individual models. Dashed red curves indicate the positions of the QHPs given by (a,e,g) Eq. (13), (b) Eq. (25), (c) Eq. (32), (d) Eq. (36), (f) Eq. (49), and (h) Eq. (56).

Accepted in ⟨ ⟩uantum 2025-12-07, click title to verify. Published under CC-BY 4.0.

9

Using the inverse transformation, we arrive at the solution for the operators $\hat{\boldsymbol{a}}$, which reads:

$$
\begin{aligned}
\hat{\boldsymbol{a}}(t) \;=\; & \boldsymbol{P}\exp(-i\boldsymbol{\Lambda^{(2)}}t)\boldsymbol{P}^{-1}\hat{\boldsymbol{a}}(0) \\
& + \int_0^t dt'\boldsymbol{P}\exp[-i\boldsymbol{\Lambda^{(2)}}(t-t')]\boldsymbol{P}^{-1}\hat{\boldsymbol{L}}(t').
\end{aligned}
\tag{17}
$$

The solution in Eq. (17) of the Heisenberg-Langevin equations in the diagonal form together with the assumption of the Gaussian Markovian character of the Langevin operator forces allows us to follow the dynamics of FOMs of an arbitrary order. We note that, from the point of view of eigenfrequencies, the FOMs of a given order form a closed dynamical system [43]. In this dynamics, we observe the genuine QEPs and QHPs that are derived from the inherited QEPs and QHPs discussed above. In general, the higher is the FOM order, the higher are the observed EDs and DDs at QEPs and QHPs. These degeneracies were systematically studied in Ref. [43] up to fourth-order FOMs. They form intricate structures within FOM spaces of defined order, where specific QEPs and QHPs emerge. Such spaces and structures can be effectively utilized to simulate various physical phenomena [49, 51]. In Appendix B, we systematically summarize these degeneracies for up to second-order FOMs, providing a comparative overview of the QEP and QHP degeneracies observed in the first- and second-order FOM dynamics.

We note that the quadratic form of Hamiltonian $\hat{H}_2$, in Eq. (1), is not the most general one. It can be extended by considering additional terms describing local squeezing in modes 1 and 2 described by a constant g, as it was done in Ref. [43]:

$$
\hat{\tilde{H}}_2 = \left[\hbar\epsilon\hat{a}_1^\dagger\hat{a}_2 + \hbar\kappa\hat{a}_1\hat{a}_2 + \sum_{j=1,2}\hbar g\hat{a}_j^{\dagger 2}/2\right] + \text{H.c.}
\tag{18}
$$

However, the structure of the dynamical matrix $\boldsymbol{M^{(2)}}$, built from the 2×2 submatrices, is broken for nonzero values of the constant g. This results in the loss of the second-order DD that follows from the structure of the $\boldsymbol{\xi}$ and $\tilde{\boldsymbol{\gamma}}_{\boldsymbol{j}}$ matrices written in Eq. (4). As a consequence, only second-order inherited QEPs occur for $g\neq 0$ in the parameter space $(\kappa/\epsilon, \gamma_-/\epsilon, g/\epsilon)$. Detailed analysis of the positions of inherited QEPs, as well as EDs and DDs of QEPs and QHPs observed in the FOMs dynamics was provided in Ref. [43]. Similar reduction of eigenvalue and eigenvector degeneracies in the Hilbert space after including these terms was observed in more complex bosonic systems. We further pay attention only to the systems described by quadratic Hamiltonians without these terms.

3 Three-mode bosonic system

The above-analyzed two-mode system provided QHPs with second-order ED and DD. Whereas the DD originates in the mutual coupling between the two modes (described by the strengths ϵ and κ), the ED arises from different strengths of damping and amplification of the modes and a given system configuration. Bosonic systems composed of more than two modes give a promise for revealing QHPs with a larger number of EDs and DDs and various configurations of the coexistence of several QHPs with different EDs and DDs. However, the question is how to choose a suitable configuration of interactions among the modes and their damping and/or amplification rates. Whereas the parity symmetry is useful in seeking promising geometries, the temporal symmetry allows to define suitable relations among the damping and amplification rates. In this section, we begin our investigation by considering three-mode bosonic systems in the linear configuration, and

define specific conditions under which QHPs occur. In the following sections, we extend our analysis to the four- and five-mode systems. The geometries together with their characteristic parameters are schematically shown in Fig. 1. We also identify the positions of QHPs in the corresponding parameter spaces. Moreover, we analyze the occurrence of genuine QEPs and QHPs and determine their EDs and DDs from the point of view of the dynamics of second-order FOMs.

Among the bosonic systems with three modes we succeeded in identifying QHPs in the linear configuration that is shown in Fig. 1(b). We note that a linear non-Hermitian Hamiltonian (i.e. semiclassical) system in a similar configuration was experimentally realized in Ref. [59] and used for higher-order exceptional-point enhanced sensing. We note that a QEP with third-order ED was identified in Ref. [60] in an optomechanical system of three interacting bosonic modes. Hamiltonian $\hat{H}_3$ of such a system can be written as follows:

$$\hat{H}_3 = \left[\hbar\epsilon\hat{a}_1^\dagger\hat{a}_2 + \hbar\epsilon\hat{a}_2^\dagger\hat{a}_3 + \hbar\kappa\hat{a}_1\hat{a}_2 + \hbar\kappa\hat{a}_2\hat{a}_3\right] + \text{H.c.} \tag{19}$$

Using the 2×2 submatrices $\tilde{\boldsymbol{\gamma}}_{\boldsymbol{j}}$, $j=1,2,3$, describing mode damping or amplification, and $\boldsymbol{\xi}$ defined in Eq. (4), we derive the Heisenberg-Langevin equations in the form

$$\frac{d\hat{\boldsymbol{a}}}{dt} = -i\boldsymbol{M}^{(\boldsymbol{3})}\hat{\boldsymbol{a}} + \hat{\boldsymbol{L}}, \tag{20}$$

where

$$\boldsymbol{M}^{(\boldsymbol{3})} = \begin{bmatrix} -i\tilde{\boldsymbol{\gamma}}_{\boldsymbol{1}} & \boldsymbol{\xi} & \boldsymbol{0} \\ \boldsymbol{\xi} & -i\tilde{\boldsymbol{\gamma}}_{\boldsymbol{2}} & \boldsymbol{\xi} \\ \boldsymbol{0} & \boldsymbol{\xi} & -i\tilde{\boldsymbol{\gamma}}_{\boldsymbol{3}} \end{bmatrix}, \tag{21}$$

and $\boldsymbol{0}$ denotes the 2×2 null matrix, while $\hat{\boldsymbol{a}} = [\hat{\boldsymbol{a}}_{\boldsymbol{1}}, \hat{\boldsymbol{a}}_{\boldsymbol{2}}, \hat{\boldsymbol{a}}_{\boldsymbol{3}}]^T \equiv \left[\hat{a}_1, \hat{a}_1^\dagger, \hat{a}_2, \hat{a}_2^\dagger, \hat{a}_3, \hat{a}_3^\dagger\right]^T$ and $\hat{\boldsymbol{L}} = \left[\hat{L}_1, \hat{L}_1^\dagger, \hat{L}_2, \hat{L}_2^\dagger, \hat{L}_3, \hat{L}_3^\dagger\right]^T$.

The condition

$$2\gamma_2 = \gamma_1 + \gamma_3 \tag{22}$$

is required to have the eigenvalues $\lambda_j^{M^{(3)}}$ $(j=1,2,3)$ of the dynamical 3×3 matrix $\boldsymbol{M}^{(\boldsymbol{3})}$ in Eq. (21) with a common damping or amplification rate γ_+. This is necessary for observing possible spectral exceptional and diabolical degeneracies.

We note that condition in Eq. (22) also encompasses passive ($\gamma_j > 0$ for $j = 1, 2, 3$) and active $\gamma_j < 0$ for $j = 1, 2, 3$ $\mathcal{PT}$-symmetric systems. Under this condition we may write

$$\lambda_1^{M^{(3)}} = -i\gamma_+, \quad \lambda_{2,3}^{M^{(3)}} = -i\gamma_+ \mp \beta, \tag{23}$$

using $4\gamma_\pm = \gamma_1 \pm \gamma_3$ and $\beta^2 = 2\xi^2 - \gamma_-^2$; ξ being an eigenvalue of the matrix $\boldsymbol{\xi}$ in Eq. (4). The eigenvectors corresponding to the eigenvalues $\lambda_j^{M^{(3)}}$ in Eq. (23) are derived in the form:

$$\boldsymbol{y}_{\boldsymbol{1}}^{\boldsymbol{M}^{(\boldsymbol{3})}} = \left[-1, -\frac{i\gamma_-}{\xi}, 1\right]^T,$$

$$\boldsymbol{y}_{\boldsymbol{2,3}}^{\boldsymbol{M}^{(\boldsymbol{3})}} = \left[1 + \frac{i\gamma_-(i\gamma_- \pm \beta)}{\xi^2}, -\frac{i\gamma_- \pm \beta}{\xi}, 1\right]^T. \tag{24}$$

Provided that $\beta = 0$, the three eigenvalues $\lambda_j^{M^{(3)}}$ for $j = 1, 2, 3$ in Eq. (23), as well as the corresponding eigenvectors in Eq. (24), are equal and, thus, third-order QEPs of the 3×3 matrix $\boldsymbol{M^{(3)}}$ are found. Taking into account the structure of the submatrices of the 6×6 matrix $\boldsymbol{M^{(3)}}$, these QEPs are in fact QHPs with second-order DD. Substituting for the eigenvalues ξ of matrix $\boldsymbol{\xi}$ from Eq. (7), the condition $\beta = \sqrt{2\zeta^2 - \gamma_-^2} = 0$ for having a QHP attains the form:

$$\frac{\kappa^2}{\epsilon^2} + \frac{\gamma_-^2}{2\epsilon^2} = 1. \tag{25}$$

This condition is visualized by the red dashed curve in Fig. 3(b) that shows the real parts of the eigenvalues $\lambda_j^{M^{(3)}}$ as they vary in the parameter space $(\kappa/\epsilon, \gamma_-/\epsilon)$.

The analysis of QEPs and QHPs appropriate for the FOM dynamics requires the construction of eigenvalues and eigenvectors of the matrix $\boldsymbol{M^{(3)}}$ in its full 6×6 space combining the eigenvalues and eigenvectors in Eqs. (23) and (24) with those of the matrix $\boldsymbol{\xi}$ given in Eqs. (7) and (8) using the general scheme shown in Fig. 2. The eigenvalues and eigenvectors are written in Appendix A. The obtained eigenvectors then allow us to introduce new field operators $\hat{\boldsymbol{b}} = \left[\hat{b}_1, \hat{b}_1^\dagger, \hat{b}_2, \hat{b}_3, \hat{b}_2^\dagger, \hat{b}_3^\dagger\right]^T$ in which the dynamical 6×6 matrix $\boldsymbol{M^{(3)}}$ of the Heisenberg-Langevin equations attains its diagonal form $\boldsymbol{\Lambda^{(3)}}$, similarly as it was done in Sec. 2 in the case of the two-mode system. This then allows to reveal the spectral degeneracies in higher-order FOMs. The QEPs and QHPs predicted in the dynamics of the first- and second-order FOMs are summarized in Appendix B using Tab. 2.

4 Four-mode bosonic systems

Let us move to the investigations of four-mode bosonic systems, in which we revealed QEPs and QHPs in two arrangements: linear and circular. In the linear arrangement, we consider two configurations that differ by the damping and/or amplification rates assigned to the modes: Either the neighbor modes share their damping and/or amplification rates or their rates differ. On the other hand, equal damping and/or amplification rates of the neighbor modes are needed in the circular arrangement to reveal QEPs and QHPs.

4.1 Linear configurations

In the linear configuration, the quadratic Hamiltonian $\hat{H}_{4,l}$ of four-mode system is expressed in the form

$$\hat{H}_{4,l} = \left[\hbar\epsilon\hat{a}_1^\dagger\hat{a}_2 + \hbar\epsilon\hat{a}_2^\dagger\hat{a}_3 + \hbar\epsilon\hat{a}_3^\dagger\hat{a}_4 + \hbar\kappa\hat{a}_1\hat{a}_2 + \hbar\kappa\hat{a}_2\hat{a}_3 + \hbar\kappa\hat{a}_3\hat{a}_4\right] + \text{H.c.} \tag{26}$$

The corresponding Heisenberg-Langevin equations are derived as follows:

$$\frac{d\hat{\boldsymbol{a}}}{dt} = -i\boldsymbol{M_l^{(4)}}\hat{\boldsymbol{a}} + \hat{\boldsymbol{L}}, \tag{27}$$

Using the 2×2 submatrices defined in Eq. (4) we write the dynamical 4×4 matrix $\boldsymbol{M_l^{(4)}}$:

$$\boldsymbol{M_l^{(4)}} = \begin{bmatrix} -i\tilde{\gamma}_1 & \boldsymbol{\xi} & \boldsymbol{0} & \boldsymbol{0} \\ \boldsymbol{\xi} & -i\tilde{\gamma}_2 & \boldsymbol{\xi} & \boldsymbol{0} \\ \boldsymbol{0} & \boldsymbol{\xi} & -i\tilde{\gamma}_3 & \boldsymbol{\xi} \\ \boldsymbol{0} & \boldsymbol{0} & \boldsymbol{\xi} & -i\tilde{\gamma}_4 \end{bmatrix}. \tag{28}$$

The vectors $\hat{\boldsymbol{a}}$ of field operators and $\hat{\boldsymbol{L}}$ of the Langevin operator forces in Eq. (27) are given as $\hat{\boldsymbol{a}} = [\hat{\boldsymbol{a}}_1, \hat{\boldsymbol{a}}_2, \hat{\boldsymbol{a}}_3, \hat{\boldsymbol{a}}_4]^T \equiv \left[\hat{a}_1, \hat{a}_1^\dagger, \hat{a}_2, \hat{a}_2^\dagger, \hat{a}_3, \hat{a}_3^\dagger, \hat{a}_4, \hat{a}_4^\dagger\right]^T$ and $\hat{\boldsymbol{L}} = \left[\hat{L}_1, \hat{L}_1^\dagger, \hat{L}_2, \hat{L}_2^\dagger, \hat{L}_3, \hat{L}_3^\dagger, \hat{L}_4, \hat{L}_4^\dagger\right]^T$.

QEPs and QHPs have been found in the following two configurations:

4.1.1 Linear configuration with equal damping and/or amplification rates of neighbor modes

In this configuration schematically shown in Fig. 1(c) we assume equal damping and/or amplification rates in modes 1 and 2, and also modes 3 and 4:

$$\gamma_1 = \gamma_2 \equiv \gamma_{12}, \qquad \gamma_3 = \gamma_4 \equiv \gamma_{34}. \tag{29}$$

In this case, diagonalization of the dynamical 4×4 matrix $\boldsymbol{M_{l1}^{(4)}}$ in Eq. (28) provides the eigenvalues

$$
\begin{aligned}
\lambda_{1,2}^{M_{l1}^{(4)}} &= -i\gamma_+ \pm \alpha_-, \\
\lambda_{3,4}^{M_{l1}^{(4)}} &= -i\gamma_+ \pm \alpha_+,
\end{aligned}
\tag{30}
$$

and the corresponding eigenvectors

$$
\begin{aligned}
\boldsymbol{y_{1,3}^{M_{l1}^{(4)}}} &= \left[-\frac{\delta_\pm^*}{2\xi^3}, \frac{\chi_\mp^{*2}}{\xi^2} - 1, \frac{\chi_\mp^*}{\xi}, 1 \right]^T, \\
\boldsymbol{y_{2,4}^{M_{l1}^{(4)}}} &= \left[\frac{\delta_\pm}{2\xi^3}, \frac{\chi_\mp^2}{\xi^2} - 1, -\frac{\chi_\mp}{\xi}, 1 \right]^T.
\end{aligned}
\tag{31}
$$

where $\delta_\pm = \xi^2(-2i\gamma_- + \chi_\mp) \pm 2\mu\chi_\mp$, $\chi_\pm = -i\gamma_+ + \alpha_\pm$, $\alpha_\pm^2 = \beta^2 \pm \mu$, $\beta^2 = 3\xi^2/2 - \gamma_-^2$, and $\mu^2 = 4\xi^2(5\xi^2/16 - \gamma_-^2)$ using $4\gamma_\pm = \gamma_{12} \pm \gamma_{34}$.

If $\mu = 0$ then $\alpha_+ = \alpha_-$ and $\chi_+ = \chi_-$. The eigenvalues in Eq. (30) are doubly degenerated: $\lambda_1^{M_{l1}^{(4)}} = \lambda_3^{M_{l1}^{(4)}}$ and $\lambda_2^{M_{l1}^{(4)}} = \lambda_4^{M_{l1}^{(4)}}$. The same holds also for their eigenvectors given in Eq. (31) and we have two QEPs with second-order ED. Similarly as in the case of three-mode bosonic system, the inclusion of the structure of submatrices in the 8×8 matrix $\boldsymbol{M_{l1}^{(4)}}$ gives the second-order DD to these QEPs and we, thus, have two QHPs. They are localized at the ellipse

$$\frac{\kappa^2}{\epsilon^2} + \frac{16\gamma_-^2}{5\epsilon^2} = 1 \tag{32}$$

defined in the parameter space $(\kappa/\epsilon, \gamma_-/\epsilon)$. Real parts of the eigenvalues $\lambda_j^{M_{l1}^{(4)}}$ for $j = 1, \ldots, 4$ are drawn in this space in Fig. 3(c); their coinciding values for the condition (32) are plotted by the red dashed curves.

The eigenvalues and eigenvectors of the 8×8 matrix $\boldsymbol{M_{l1}^{(4)}}$ obtained by merging those written in Eqs. (30) and (31) and Eqs. (7) and (8) for the matrix $\boldsymbol{\xi}$ (for details, see Appendix A) using the scheme in Fig. 2 define the transformation into the new field operators $\hat{\boldsymbol{b}} = \left[\hat{b}_1, \hat{b}_2, \hat{b}_1^\dagger, \hat{b}_2^\dagger, \hat{b}_3, \hat{b}_4, \hat{b}_3^\dagger, \hat{b}_4^\dagger \right]^T$ in which the Heisenberg-Langevin equations have the diagonal form. This reveals the spectral degeneracies in higher-order FOMs that are summarized in Tab. 3 in Appendix B considering the first- and second-order FOMs.

4.1.2 Linear configuration with different damping and/or amplification rates for neighbor modes

We assume the equal damping and/or amplification rates in modes 1 and 3 and also in modes 2 and 4:

$$\gamma_1 = \gamma_3 \equiv \gamma_{13}, \qquad \gamma_2 = \gamma_4 \equiv \gamma_{24}. \tag{33}$$

In this configuration, which is schematically depicted in Fig. 1(e), the eigenvalues of the 4×4 dynamical matrix $\boldsymbol{M_{12}^{(4)}}$ are obtained as follows:

$$
\begin{aligned}
\lambda_{1,2}^{M_{12}^{(4)}} &= -i\gamma_+ \pm \alpha_+, \\
\lambda_{3,4}^{M_{12}^{(4)}} &= -i\gamma_+ \pm \alpha_-.
\end{aligned}
\tag{34}
$$

The corresponding eigenvectors are reached in the form:

$$
\begin{aligned}
\boldsymbol{y_{1,3}^{M_{12}^{(4)}}} &= \left[\frac{-\kappa_\mp}{\xi}, \kappa_\pm, \frac{\chi_\pm^*}{\xi}, 1 \right]^T, \\
\boldsymbol{y_{2,4}^{M_{12}^{(4)}}} &= \left[\frac{\kappa_\mp \chi_\pm}{\xi}, \kappa_\pm, -\frac{\chi_\pm}{\xi}, 1 \right]^T,
\end{aligned}
\tag{35}
$$

where $\kappa_\pm = (\pm\sqrt{5}+1)/2$, $\chi_\pm = -i\gamma_+ + \alpha_\pm$, $\alpha_\pm^2 = \tilde{\beta} \pm \mu$, $\tilde{\beta} = 3\xi^2/2 - \gamma_-^2$, and $\mu = \sqrt{5}\xi^2/2$ using $4\gamma_\pm = \gamma_{13} \pm \gamma_{24}$.

Provided that $\alpha_+ = 0$ [$\alpha_- = 0$] the eigenvalues $\lambda_1^{M_{12}^{(4)}}$ and $\lambda_2^{M_{12}^{(4)}}$ [$\lambda_3^{M_{12}^{(4)}}$ and $\lambda_4^{M_{12}^{(4)}}$] in Eq. (34) and the eigenvectors $\boldsymbol{y_1^{M_{12}^{(4)}}}$ and $\boldsymbol{y_2^{M_{12}^{(4)}}}$ [$\boldsymbol{y_3^{M_{12}^{(4)}}}$ and $\boldsymbol{y_4^{M_{12}^{(4)}}}$] in Eq. (35) are equal to each other and we have a QEP with second-order ED. This means that, for the 8×8 dynamical matrix $\boldsymbol{M_{12}^{(4)}}$, we predict a QHP with second-order ED and DD observed either for $\alpha_+ = 0$ or $\alpha_- = 0$. These conditions define two ellipses in the parameter space $(\kappa/\epsilon, \gamma_-/\epsilon)$,

$$
\frac{\kappa^2}{\epsilon^2} + \frac{2\gamma_-^2}{(3 \pm \sqrt{5})\epsilon^2} = 1.
\tag{36}
$$

They are shown in Fig. 3(d) where the real parts of the eigenvalues $\lambda_j^{M_{12}^{(4)}}$ for $j = 1, \ldots, 4$ are plotted; they are drawn by the red dashed curves for the condition in Eq. (36).

The eigenvalues and eigenvectors of the 8×8 matrix $\boldsymbol{M_{12}^{(4)}}$, given in Appendix A, determine the transformation that leaves the Heisenberg-Langevin equations in their diagonal form. Thus, we define the new field operators $\hat{\boldsymbol{b}} = \left[\hat{b}_1, \hat{b}_2, \hat{b}_1^\dagger, \hat{b}_2^\dagger, \hat{b}_3, \hat{b}_4, \hat{b}_3^\dagger, \hat{b}_4^\dagger \right]^T$, whose evolution allows to identify the QEPs and QHPs in the first- and second-order FOM dynamics. They are given in Tab. 4 of Appendix B.

4.2 Circular configuration

In the circular configuration, the Hamiltonian $\hat{H}_{4,c}$ of four-mode system is expressed as

$$
\begin{aligned}
\hat{H}_{4,c} &= \left[\hbar\epsilon\hat{a}_1^\dagger\hat{a}_2 + \hbar\epsilon\hat{a}_2^\dagger\hat{a}_3 + \hbar\epsilon\hat{a}_3^\dagger\hat{a}_4 + \hbar\epsilon\hat{a}_4^\dagger\hat{a}_1 + \hbar\kappa\hat{a}_1\hat{a}_2 \right. \\
&\quad \left. +\hbar\kappa\hat{a}_2\hat{a}_3 + \hbar\kappa\hat{a}_3\hat{a}_4 + \hbar\kappa\hat{a}_4\hat{a}_1 \right] + \text{H.c.}
\end{aligned}
\tag{37}
$$

Whereas the Heisenberg-Langevin equations keep the form of Eq. (27), the original dynamical 4×4 matrix $\boldsymbol{M_l^{(4)}}$ of the linear configuration in Eq. (28) is modified into the form

$$
\boldsymbol{M_c^{(4)}} = \begin{bmatrix} -i\tilde{\gamma}_1 & \xi & 0 & \xi \\ \xi & -i\tilde{\gamma}_2 & \xi & 0 \\ 0 & \xi & -i\tilde{\gamma}_3 & \xi \\ \xi & 0 & \xi & -i\tilde{\gamma}_4 \end{bmatrix}.
\tag{38}
$$

We derive the eigenvalues of the 4×4 matrix $\boldsymbol{M_c^{(4)}}$ under the condition of the equal damping and/or amplification rates of the neighbor modes valid for the configuration plotted in Fig. 1(d); i.e.,

$$\gamma_1 = \gamma_2 \equiv \gamma_{12}, \qquad \gamma_3 = \gamma_4 \equiv \gamma_{34}. \tag{39}$$

We obtain the following eigenvalues

$$\begin{aligned}
\lambda_{1,2}^{M_{c1}^{(4)}} &= -i\gamma_+ - \alpha_\pm, \\
\lambda_{3,4}^{M_{c1}^{(4)}} &= -i\gamma_+ + \alpha_\mp
\end{aligned} \tag{40}$$

that are accompanied by the following eigenvectors

$$\begin{aligned}
\boldsymbol{y_{1,2}^{M_{c1}^{(4)}}} &= \left[-\frac{\chi}{\xi}, \pm\frac{\chi}{\xi}, \mp 1, 1 \right]^T, \\
\boldsymbol{y_{3,4}^{M_{c1}^{(4)}}} &= \left[\frac{\chi^*}{\xi}, \mp\frac{\chi^*}{\xi}, \mp 1, 1 \right]^T.
\end{aligned} \tag{41}$$

The symbols introduced in Eqs. (40) and (41) are defined as $\chi = i\gamma_+ + \beta$, $\alpha_\pm = \beta \pm \xi$, $\beta^2 = \xi^2 - \gamma_-^2$, and $4\gamma_\pm = \gamma_{12} \pm \gamma_{34}$.

For $\beta = 0$, we have $\alpha_+ = -\alpha_-$ and $\chi^* = -\chi$. This leads to the relations $\lambda_1^{M_{c1}^{(4)}} = \lambda_3^{M_{c1}^{(4)}}$ and $\lambda_2^{M_{c1}^{(4)}} = \lambda_4^{M_{c1}^{(4)}}$. Also the corresponding eigenvectors coincide: $\boldsymbol{y_1^{M_{c1}^{(4)}}} = \boldsymbol{y_3^{M_{c1}^{(4)}}}$ and $\boldsymbol{y_2^{M_{c1}^{(4)}}} = \boldsymbol{y_4^{M_{c1}^{(4)}}}$. As a consequence, the two QEPs with second-order EDs occur. This means that the two QHPs with second-order EDs and DDs for the 8×8 matrix $\boldsymbol{M_{c1}^{(4)}}$ are formed. These QHPs occur under the condition specified in Eq. (13) that identifies the QHPs in the analyzed two-mode bosonic system. The real values of the eigenvalues $\lambda_j^{M_{c1}^{(4)}}$ for $j = 1, \ldots, 4$ are plotted in Fig. 3(e) together with the condition for the QHPs; the red dashed curves give the coinciding values under the condition in Eq. (13).

Using the eigenvalues and eigenvectors of the 4×4 matrix $\boldsymbol{M_{c1}^{(4)}}$ and the 2×2 matrix $\boldsymbol{\xi}$ given in Eqs. (40), (41), (7), and (8), we arrive at the system dynamical matrix in its diagonal form (for details, see Appendix A). This brings us the new field operators $\hat{\boldsymbol{b}} = \left[\hat{b}_1, \hat{b}_2, \hat{b}_3^\dagger, \hat{b}_4^\dagger, \hat{b}_3, \hat{b}_4, \hat{b}_1^\dagger, \hat{b}_2^\dagger \right]^T$ suitable for revealing QEPs and QHPs found in the dynamics of FOMs. As the structure of eigenvalues and eigenvectors is the same as that characterizing the four-mode linear system with equal damping and/or amplification rates of neighbor modes, the appropriate QEPs and QHPs are given in Tab. 3 in Appendix B.

5 Five-mode bosonic systems

The largest bosonic systems in our investigations consist of five bosonic modes. Among them, QEPs and QHPs were identified in two configurations: linear and pyramid.

5.1 Linear configuration

A five-mode bosonic system in its linear configuration is depicted in Fig. 1(f). Its Hamiltonian $\hat{H}_{5,l}$ is given as follows:

$$\begin{aligned}
\hat{H}_{5,l} &= \left[\hbar\epsilon \hat{a}_1^\dagger \hat{a}_2 + \hbar\epsilon \hat{a}_2^\dagger \hat{a}_3 + \hbar\epsilon \hat{a}_3^\dagger \hat{a}_4 + \hbar\epsilon \hat{a}_4^\dagger \hat{a}_5 + \hbar\kappa \hat{a}_1 \hat{a}_2 \right. \\
&\quad \left. + \hbar\kappa \hat{a}_2 \hat{a}_3 + \hbar\kappa \hat{a}_3 \hat{a}_4 + \hbar\kappa \hat{a}_4 \hat{a}_5 \right] + \text{H.c.}
\end{aligned} \tag{42}$$

Defining the vectors $\hat{\boldsymbol{a}} = [\hat{\boldsymbol{a}}_1, \hat{\boldsymbol{a}}_2, \hat{\boldsymbol{a}}_3, \hat{\boldsymbol{a}}_4, \hat{\boldsymbol{a}}_5]^T \equiv \left[\hat{a}_1, \hat{a}_1^\dagger, \hat{a}_2, \hat{a}_2^\dagger, \hat{a}_3, \hat{a}_3^\dagger, \hat{a}_4, \hat{a}_4^\dagger, \hat{a}_5, \hat{a}_5^\dagger\right]^T$ of field operators and $\hat{\boldsymbol{L}} = \left[\hat{L}_1, \hat{L}_1^\dagger, \hat{L}_2, \hat{L}_2^\dagger, \hat{L}_3, \hat{L}_3^\dagger, \hat{L}_4, \hat{L}_4^\dagger, \hat{L}_5, \hat{L}_5^\dagger\right]^T$ of the Langevin operator forces, we obtain the following Heisenberg-Langevin equations:

$$\frac{d\hat{\boldsymbol{a}}}{dt} = -i\boldsymbol{M}_{\mathbf{l}}^{(5)}\hat{\boldsymbol{a}} + \hat{\boldsymbol{L}}. \tag{43}$$

The dynamical 10×10 matrix $\boldsymbol{M}_{\mathbf{l}}^{(5)}$ introduced in Eq. (43) is written with the help of 2×2 submatrices introduced in Eq. (4) as

$$\boldsymbol{M}_{\mathbf{l}}^{(5)} = \begin{bmatrix} -i\tilde{\gamma}_{\mathbf{1}} & \boldsymbol{\xi} & \mathbf{0} & \mathbf{0} & \mathbf{0} \\ \boldsymbol{\xi} & -i\tilde{\gamma}_{\mathbf{2}} & \boldsymbol{\xi} & \mathbf{0} & \mathbf{0} \\ \mathbf{0} & \boldsymbol{\xi} & -i\tilde{\gamma}_{\mathbf{3}} & \boldsymbol{\xi} & \mathbf{0} \\ \mathbf{0} & \mathbf{0} & \boldsymbol{\xi} & -i\tilde{\gamma}_{\mathbf{4}} & \boldsymbol{\xi} \\ \mathbf{0} & \mathbf{0} & \mathbf{0} & \boldsymbol{\xi} & -i\tilde{\gamma}_{\mathbf{5}} \end{bmatrix}. \tag{44}$$

Motivated by $\mathcal{PT}$ symmetry we assume:

$$\gamma_1 = \gamma_2 \equiv \gamma_{12}, \qquad \gamma_4 = \gamma_5 \equiv \gamma_{45}. \tag{45}$$

Moreover, inspired by the condition in Eq. (22) derived for the three-mode linear system, we additionally assume:

$$2\gamma_3 = \gamma_{12} + \gamma_{45}. \tag{46}$$

Then, diagonalization of the 5×5 matrix $\boldsymbol{M}_{\mathbf{l}}^{(5)}$ results in the following eigenvalues $\lambda_j^{M_{\mathbf{l}}^{(5)}}$:

$$\begin{aligned} \lambda_1^{M_{\mathbf{l}}^{(5)}} &= -i\gamma_+, \\ \lambda_{2,3}^{M_{\mathbf{l}}^{(5)}} &= -i\gamma_+ \pm \alpha_-, \\ \lambda_{4,5}^{M_{\mathbf{l}}^{(5)}} &= -i\gamma_+ \pm \alpha_+. \end{aligned} \tag{47}$$

The corresponding eigenvectors are derived as follows:

$$\begin{aligned} \boldsymbol{y}_{\mathbf{1}}^{M_{\mathbf{l}}^{(5)}} &= \left[1, \frac{i\gamma_-}{\xi}, -\frac{\gamma_-^2}{\xi^2} - 1, -\frac{i\gamma_-}{\xi}, 1\right]^T, \\ \boldsymbol{y}_{\mathbf{2},\mathbf{4}}^{M_{\mathbf{l}}^{(5)}} &= \left[-1 \mp \frac{n_\mp}{4\xi^3}, -\frac{m_\mp}{\xi^3} \mp \frac{2\beta\chi_\mp}{\xi^2}, \frac{\chi_\mp^2}{\xi^2} - 1, \frac{\chi_\mp}{\xi}, 1\right]^T, \\ \boldsymbol{y}_{\mathbf{3},\mathbf{5}}^{M_{\mathbf{l}}^{(5)}} &= \left[-1 \mp \frac{n_\mp^*}{4\xi^3}, \frac{m_\mp^*}{\xi^3} \pm \frac{2\beta\chi_\mp^*}{\xi^2}, \frac{\chi_\mp^{*2}}{\xi^2} - 1, -\frac{\chi_\mp^*}{\xi}, 1\right]^T, \end{aligned} \tag{48}$$

where $n_\mp = (2\beta \mp \xi)[(2\beta \mp \xi)^2 - 4i\gamma_-\alpha_\mp]$, $m_\mp = i\gamma_-(\chi_\mp^2 + \xi^2)$, $\chi_\pm = -i\gamma_+ + \alpha_\pm$, $\alpha_\pm^2 = \beta^2 + 7\xi^2/4 \pm 2\beta\xi$, $\beta^2 = \xi^2/4 - \gamma_-^2$, and $4\gamma_\pm = \gamma_{12} \pm \gamma_{45}$.

If $\beta = 0$ then $\alpha_+ = \alpha_-$ and $\chi_+ = \chi_-$. Under these conditions, we have $\lambda_2^{M_{\mathbf{l}}^{(5)}} = \lambda_4^{M_{\mathbf{l}}^{(5)}}$ and $\boldsymbol{y}_{\mathbf{2}}^{M_{\mathbf{l}}^{(5)}} = \boldsymbol{y}_{\mathbf{4}}^{M_{\mathbf{l}}^{(5)}}$. We also have $\lambda_3^{M_{\mathbf{l}}^{(5)}} = \lambda_5^{M_{\mathbf{l}}^{(5)}}$ and $\boldsymbol{y}_{\mathbf{3}}^{M_{\mathbf{l}}^{(5)}} = \boldsymbol{y}_{\mathbf{5}}^{M_{\mathbf{l}}^{(5)}}$. Thus, we observe two QEPs with second-order EDs that give rise to two QHPs with second-order EDs and

DDs when the 10×10 matrix $\boldsymbol{M_1^{(5)}}$ is analyzed. In the parameter space $(\kappa/\epsilon, \gamma_-/\epsilon)$, these QHPs are localized at the positions obeying the condition

$$\frac{\kappa^2}{\epsilon^2} + \frac{4\gamma_-^2}{\epsilon^2} = 1. \tag{49}$$

The real parts of the eigenvalues $\lambda_j^{M_1^{(5)}}$ forming QHPs ($j = 2, \ldots, 5$) are plotted in Fig. 3(f) where their coinciding values for the condition in Eq. (49) are indicated by the red dashed curves.

The eigenvalues and eigenvectors of the 10×10 matrix $\boldsymbol{M_1^{(5)}}$ constructed from the formulas given in Eqs. (47) and (48) together with those in Eqs. (7) and (8) (for details, see Appendix A) allow us to describe the system dynamics via a diagonal dynamical matrix. The appropriate operators $\hat{\boldsymbol{b}} = \left[\hat{b}_1, \hat{b}_1^\dagger, \hat{b}_2, \hat{b}_3, \hat{b}_2^\dagger, \hat{b}_3^\dagger, \hat{b}_4, \hat{b}_5, \hat{b}_4^\dagger, \hat{b}_5^\dagger\right]^T$ then reveal QEPs and QHPs found in the dynamics of FOMs of different orders. For the first- and second-order FOMs they are written in Tab. 5 of Appendix B.

5.2 Pyramid configuration

Second-order QEPs and QHPs can also be identified in the pyramid configuration [the only considered non-planar configuration, see Fig. 1(g)] described by the following Hamiltonian $\hat{H}_{5,\mathrm{p}}$:

$$\begin{aligned}
\hat{H}_{5,\mathrm{p}} &= \left[\hbar\epsilon\hat{a}_1^\dagger\hat{a}_2 + \hbar\epsilon\hat{a}_1^\dagger\hat{a}_4 + \hbar\epsilon\hat{a}_1^\dagger\hat{a}_5 + \hbar\epsilon\hat{a}_2^\dagger\hat{a}_3 + \hbar\epsilon\hat{a}_2^\dagger\hat{a}_5 + \hbar\epsilon\hat{a}_3^\dagger\hat{a}_4 + \hbar\epsilon\hat{a}_3^\dagger\hat{a}_5 \right. \\
&\quad + \hbar\epsilon\hat{a}_4^\dagger\hat{a}_5 + \hbar\kappa\hat{a}_1\hat{a}_2 + \hbar\kappa\hat{a}_1\hat{a}_4 + \hbar\kappa\hat{a}_1\hat{a}_5 + \hbar\kappa\hat{a}_2\hat{a}_3 + \hbar\kappa\hat{a}_2\hat{a}_5 \\
&\quad \left. + \hbar\kappa\hat{a}_3\hat{a}_4 + \hbar\kappa\hat{a}_3\hat{a}_5 + \hbar\kappa\hat{a}_4\hat{a}_5\right] + \mathrm{H.c.}
\end{aligned} \tag{50}$$

The Hamiltonian $\hat{H}_{5,\mathrm{p}}$ given in Eq. (50) leads to the Heisenberg-Langevin equations (43) in which the dynamical 10×10 matrix $\boldsymbol{M_\mathrm{p}^{(5)}}$ attains the form using the 2×2 sub-matrices introduced in Eq. (4):

$$\boldsymbol{M_\mathrm{p}^{(5)}} = \begin{bmatrix} -i\tilde{\gamma}_1 & \xi & 0 & \xi & \xi \\ \xi & -i\tilde{\gamma}_2 & \xi & 0 & \xi \\ 0 & \xi & -i\tilde{\gamma}_3 & \xi & \xi \\ \xi & 0 & \xi & -i\tilde{\gamma}_4 & \xi \\ \xi & \xi & \xi & \xi & -i\tilde{\gamma}_5 \end{bmatrix}. \tag{51}$$

Motivated by the $\mathcal{PT}$ symmetry we assume:

$$\gamma_1 = \gamma_2 \equiv \gamma_{12}, \qquad \gamma_3 = \gamma_4 \equiv \gamma_{34}. \tag{52}$$

Moreover, inspired by the condition (22) derived for the three-mode linear bosonic system, we additionally assume:

$$2\gamma_5 = \gamma_{12} + \gamma_{34}. \tag{53}$$

Under these conditions, diagonalization of the 5×5 matrix $\boldsymbol{M_\mathrm{p}^{(5)}}$ leaves us the following five eigenvalues $\lambda_j^{M_\mathrm{p}^{(5)}}$:

$$\begin{aligned}
\lambda_1^{M^{(5)\mathrm{p}}} &= -i\gamma_+, \\
\lambda_{2,3}^{M_\mathrm{p}^{(5)}} &= -i\gamma_+ - \xi \pm \beta_1, \\
\lambda_{4,5}^{M_\mathrm{p}^{(5)}} &= -i\gamma_+ + \xi \pm \beta_2.
\end{aligned} \tag{54}$$

The corresponding eigenvectors are obtained as follows:

$$
\begin{aligned}
\boldsymbol{y_1}^{M_{\mathrm{p}}^{(5)}} &= \left[\frac{-i\xi}{\gamma_-}, \frac{-i\xi}{\gamma_-}, \frac{i\xi}{\gamma_-}, \frac{i\xi}{\gamma_-}, 1\right]^T, \\
\boldsymbol{y_2}^{M_{\mathrm{p}}^{(5)}} &= \left[\frac{\chi_1}{\xi}, -\frac{\chi_1}{\xi}, -1, 1, 0\right]^T, \\
\boldsymbol{y_3}^{M_{\mathrm{p}}^{(5)}} &= \left[-\frac{\chi_1^*}{\xi}, \frac{\chi_1^*}{\xi}, -1, 1, 0\right]^T, \\
\boldsymbol{y_4}^{M_{\mathrm{p}}^{(5)}} &= \left[\sigma_+, \sigma_+, \sigma_+^*, \sigma_+^*, 1\right]^T, \\
\boldsymbol{y_5}^{M_{\mathrm{p}}^{(5)}} &= \left[\sigma_-^*, \sigma_-^*, \sigma_-, \sigma_-, 1\right]^T,
\end{aligned}
\tag{55}
$$

where $\sigma_\pm = (\xi \pm \chi_2)/(4\xi)$, $\beta_1^2 = \xi^2 - \gamma_-^2$, $\beta_2^2 = 5\xi^2 - \gamma_-^2$, $\chi_{1,2} = \beta_{1,2} - i\gamma_-$, and $4\gamma_\pm = \gamma_{12} \pm \gamma_{34}$.

Contrary to the eigenvalues of the models discussed above, the eigenvalues $\lambda_j^{M_{\mathrm{p}}^{(5)}}$ for $j = 2, \ldots, 5$ in Eq. (55) exhibit the linear dependence on ξ. This means that the DD inherited to all the above-discussed models is removed in this model. It remains only for the eigenvalue $\lambda_1^{M_{\mathrm{p}}^{(5)}}$ that, however, has no ability to form EDs.

Provided that $\beta_1 = 0$, we have $\lambda_2^{M_{\mathrm{p}}^{(5)}} = \lambda_3^{M_{\mathrm{p}}^{(5)}}$ and $\boldsymbol{y_2}^{M_{\mathrm{p}}^{(5)}} = \boldsymbol{y_3}^{M_{\mathrm{p}}^{(5)}}$. Thus, we have the QEP with second-order ED. When the 10×10 matrix $\boldsymbol{M_{\mathrm{p}}^{(5)}}$ is analyzed, there occur one second-order QEP for $\xi = \zeta$ and one second-order QEP for $\xi = -\zeta$. These QEPs occur in the parameter space $(\kappa/\epsilon, \gamma_-/\epsilon)$ under the condition written in Eq. (13).

Moreover, in parallel, if $\beta_2 = 0$, it holds that $\lambda_4^{M_{\mathrm{p}}^{(5)}} = \lambda_5^{M_{\mathrm{p}}^{(5)}}$ and $\boldsymbol{y_4}^{M_{\mathrm{p}}^{(5)}} = \boldsymbol{y_5}^{M_{\mathrm{p}}^{(5)}}$. Thus, similarly as above, we observe the QEP with second-order ED for the 5×5 matrix $\boldsymbol{M_{\mathrm{p}}^{(5)}}$. There occur one second-order QEP for $\xi = \zeta$ and one second-order QEP for $\xi = -\zeta$ for the 10×10 matrix $\boldsymbol{M_{\mathrm{p}}^{(5)}}$. These QEPs are localized in the parameter space $(\kappa/\epsilon, \gamma_-/\epsilon)$ at the points fulfilling the condition:

$$
\frac{\kappa^2}{\epsilon^2} + \frac{\gamma_-^2}{5\epsilon^2} = 1.
\tag{56}
$$

The real parts of the eigenvalues $\lambda_j^{M_{\mathrm{p}}^{(5)}}$ forming QEPs ($j = 2, \ldots, 5$) are drawn in Fig. 3(g,h); the coinciding values occurring for the condition in Eq. (13) [(56)] are plotted in Fig. 3(g) [(h)] as red dashed curves.

We note that for $\xi = 0$ (i.e., $\gamma_- = 0$, $\kappa = \epsilon$) we have a specific QHP with ten-fold frequency degeneracy that belongs to four doubly-degenerate eigenvectors and another two eigenvectors.

The eigenvalues and eigenvectors of the 10×10 matrix $\boldsymbol{M_{\mathrm{p}}^{(5)}}$ formed from the expressions given in Eqs. (54) and (55) and also in Eqs. (7) and (8) (for details, see Appendix A) using the scheme in Fig. 2 allow us to analyze the system dynamics via a diagonal dynamical matrix. The appropriate operators $\hat{\boldsymbol{b}} = \left[\hat{b}_1, \hat{b}_1^\dagger, \hat{b}_2, \hat{b}_3, \hat{b}_3^\dagger, \hat{b}_2^\dagger, \hat{b}_4, \hat{b}_5, \hat{b}_5^\dagger, \hat{b}_4^\dagger\right]^T$ then allow to identify the QEPs and QHPs observed in the dynamics of FOMs of different orders. For the first- and second-order FOMs, they are explicitly given in Tab. 6 in Appendix B.

6 Conclusions

We have analyzed the dynamics of simple bosonic systems described by quadratic non-Hermitian Hamiltonians from the point of view of the occurrence of quantum exceptional, diabolical, and hybrid points. Non-Hermiticity of the considered systems, composed of from two to five coupled modes, originated in their damping and/or amplification, that are accompanied by the corresponding Langevin fluctuating forces to assure the physically consistent behavior. We have identified specific configurations defined by two-mode couplings and conditions for the damping and amplification rates of the modes at which the inherited quantum exceptional and diabolical points occur. Surprisingly, in these physically consistent models, we have found only second- and third-order inherited quantum exceptional points including their doubling due to second-order diabolical degeneracies. On the other hand, doubled second-order inherited quantum exceptional points have been observed. We have shown that the analyzed bosonic systems naturally exhibit the second-order diabolical degeneracies. Nevertheless, we have found an exception from this behavior in which no diabolical degeneracy occurs.

The exceptional and diabolical degeneracies of inherited quantum hybrid points have then been used to construct higher-order degeneracies observed in the dynamics of second-order field-operator moments. The corresponding quantum exceptional and hybrid points are summarized in tables that demonstrate richness of the evolution of the general-order field-operator moments and serve for future studies of the related physical effects.

The investigations have revealed the need for further looking for the bosonic systems exhibiting higher-order inherited quantum exceptional and hybrid points by considering more general bosonic systems. In Ref. [50] we extend our investigations to the systems with partial $\mathcal{PT}$-symmetry like dynamics (nonconventional $\mathcal{PT}$-symmetry) as well as non-Hermitian bosonic systems with unidirectional coupling.

We may conclude in general that the performed analysis opens the door for further detailed investigations of the role of exceptional and diabolical degeneracies responsible for inducing unusual physical effects observed in physically well-behaved systems at exceptional, diabolical, and hybrid points.

7 Acknowledgements

A Eigenvalues and eigenvectors of three-, four- and five-mode bosonic systems

In this Appendix, we present the eigenvalues and eigenvectors of the dynamical matrices of the Heisenberg-Langevin equations for the three-, four-, and five-mode bosonic systems in configurations depicted in Fig. 1.

A.1 General n-mode bosonic systems

The eigenvalues of the $2n \times 2n$ dynamical matrix $\boldsymbol{M^{(n)}}$ belonging to a system with n modes ($n = 2, 3, \ldots$) are constructed from the eigenvalues $\lambda_j^{M^{(n)}}$, $j = 1, \ldots, n$, derived for the form of the dynamical matrix containing 2×2 submatrices and the eigenvalues λ_j^ξ, $j = 1, 2$, of the matrix $\boldsymbol{\xi}$ given in Eq. (7) as follows:

$$
\begin{aligned}
\Lambda_{2j-1}^{M^{(n)}} &= \lambda_j^{M^{(n)}}(\xi = \lambda_1^\xi), \\
\Lambda_{2j}^{M^{(n)}} &= \lambda_j^{M^{(n)}}(\xi = \lambda_2^\xi), \quad j = 1, 2, \ldots, n.
\end{aligned} \tag{57}
$$

Similarly, using the corresponding eigenvectors $\boldsymbol{y_j^{M^{(n)}}}$ of the $n \times n$ matrix $\boldsymbol{M^{(n)}}$ formed by submatrices and the eigenvectors $\boldsymbol{y_j^\xi}$, $j = 1, 2$, of the matrix $\boldsymbol{\xi}$ in Eq. (8), we arrive at the following eigenvectors of the $2n \times 2n$ matrix $\boldsymbol{M^{(n)}}$ associated with the eigenvalues given in Eq. (57):

$$
\begin{aligned}
\boldsymbol{Y_{2j-1}^{M^{(n)}}} &= \begin{bmatrix} y_{j,1}^{M^{(n)}}(\xi = \lambda_1^\xi)\boldsymbol{y_1^\xi} \\ y_{j,2}^{M^{(n)}}(\xi = \lambda_1^\xi)\boldsymbol{y_1^\xi} \\ \ldots \\ y_{j,n}^{M^{(n)}}(\xi = \lambda_1^\xi)\boldsymbol{y_1^\xi} \end{bmatrix}, \\
\boldsymbol{Y_{2j}^{M^{(n)}}} &= \begin{bmatrix} y_{j,1}^{M^{(n)}}(\xi = \lambda_2^\xi)\boldsymbol{y_2^\xi} \\ y_{j,2}^{M^{(n)}}(\xi = \lambda_2^\xi)\boldsymbol{y_2^\xi} \\ \ldots \\ y_{j,n}^{M^{(n)}}(\xi = \lambda_2^\xi)\boldsymbol{y_2^\xi} \end{bmatrix}, \quad j = 1, \ldots, n.
\end{aligned} \tag{58}
$$

A.2 Three-mode bosonic system

In the three-mode system ($n = 3$) assuming $\beta = \sqrt{2\zeta^2 - \gamma_-^2} = 0$, we find a QHP with third-order ED and second-order DD. All the eigenvalues in Eq. (57) are the same in this case and the eigenvectors in Eq. (58) obey the relations $\boldsymbol{Y_1^{M^{(3)}}} = \boldsymbol{Y_3^{M^{(3)}}} = \boldsymbol{Y_5^{M^{(3)}}}$ and $\boldsymbol{Y_2^{M^{(3)}}} = \boldsymbol{Y_4^{M^{(3)}}} = \boldsymbol{Y_6^{M^{(3)}}}$.

A.3 Four-mode bosonic systems

In the four-mode system ($n = 4$) in the linear configuration with equal damping and/or amplification rates of neighbor modes and assuming $\mu = 2\sqrt{\zeta^2(5\zeta^2/16 - \gamma_-^2)} = 0$, we observe two QHPs with second-order ED and second-order DD. The eigenvalues $\Lambda_{1,2,5,6}^{M_{11}^{(4)}}$ and also the eigenvalues $\Lambda_{3,4,7,8}^{M_{11}^{(4)}}$ in Eq. (57) coincide. The eigenvectors in Eq. (58) obey the relations $\boldsymbol{Y_j^{M_{11}^{(4)}}} = \boldsymbol{Y_{j+4}^{M_{11}^{(4)}}}$ for $j = 1, \ldots, 4$.

In the four-mode system ($n = 4$) in the linear configuration with different damping and/or amplification rates in neighbor modes and assuming $\alpha_+ = 0$ [$\alpha_- = 0$], $\alpha_\pm = \sqrt{(3 \pm \sqrt{5})\zeta^2/2 - \gamma_-^2)} = 0$, we find a single QHP with second-order ED and DD. The eigenvalues $\Lambda_{1,2,3,4}^{M_{12}^{(4)}}$ [$\Lambda_{5,6,7,8}^{M_{12}^{(4)}}$] in Eq. (57) are equal. The eigenvectors in Eq. (58) fulfil: $\boldsymbol{Y_1^{M_{12}^{(4)}}} = \boldsymbol{Y_3^{M_{13}^{(4)}}}$ and $\boldsymbol{Y_2^{M_{12}^{(4)}}} = \boldsymbol{Y_4^{M_{12}^{(4)}}}$ [$\boldsymbol{Y_5^{M_{12}^{(4)}}} = \boldsymbol{Y_7^{M_{12}^{(4)}}}$ and $\boldsymbol{Y_6^{M_{12}^{(4)}}} = \boldsymbol{Y_8^{M_{12}^{(4)}}}$].

In the four-mode system ($n = 4$) in the circular configuration with equal damping and/or amplification rates of neighbor modes and assuming $\beta = \sqrt{\zeta^2 - \gamma_-^2} = 0$, we have

two QHPs with second-order EDs and second-order DDs. The eigenvalues and eigenvectors in this case behave analogous to those given above for the four-mode system in the linear configuration with equal damping and/or amplification rates of neighbor modes.

A.4 Five-mode bosonic systems

In the five-mode system ($n = 5$) in the linear configuration and assuming $\beta = \sqrt{\zeta^2/4 - \gamma_-^2} = 0$, we have two QHPs with second-order EDs and second-order DDs. The eigenvalues $\Lambda_{3,4,7,8}^{M_1^{(5)}}$ and also the eigenvalues $\Lambda_{5,6,9,10}^{M_1^{(5)}}$ in Eq. (57) are the same. The eigenvectors in Eq. (58) fulfill the relations: $\boldsymbol{Y_3}^{M_1^{(5)}} = \boldsymbol{Y_7}^{M_1^{(5)}}$, $\boldsymbol{Y_4}^{M_1^{(5)}} = \boldsymbol{Y_8}^{M_1^{(5)}}$, $\boldsymbol{Y_5}^{M_1^{(5)}} = \boldsymbol{Y_9}^{M_1^{(5)}}$, and $\boldsymbol{Y_6}^{M_1^{(5)}} = \boldsymbol{Y_{10}}^{M_1^{(5)}}$.

In the five-mode system ($n = 5$) in the pyramid configuration and assuming $\beta_1 = \sqrt{\zeta^2 - \gamma_-^2} = 0$, we have two QEPs with second-order ED. The eigenvalues $\Lambda_3^{M_p^{(5)}}$ and $\Lambda_5^{M_p^{(5)}}$ together with their accompanying eigenvectors $\boldsymbol{Y_3}^{M_p^{(5)}} = \boldsymbol{Y_5}^{M_p^{(5)}}$ coincide. The same is true for eigenvalues $\Lambda_4^{M_p^{(5)}}$ and $\Lambda_6^{M_p^{(5)}}$ and eigenvectors $\boldsymbol{Y_4}^{M_p^{(5)}}$ and $\boldsymbol{Y_6}^{M_p^{(5)}}$. Provided that $\beta_2 = \sqrt{5\zeta^2 - \gamma_-^2} = 0$, we reveal two QEPs with second-order ED. The eigenvalues $\Lambda_7^{M_p^{(5)}}$ and $\Lambda_9^{M_p^{(5)}}$ together with their accompanying eigenvectors $\boldsymbol{Y_7}^{M_p^{(5)}}$ and $\boldsymbol{Y_9}^{M_p^{(5)}}$ are the same. Similarly, the eigenvalues $\Lambda_8^{M_p^{(5)}}$ and $\Lambda_{10}^{M_p^{(5)}}$ and eigenvectors $\boldsymbol{Y_8}^{M_p^{(5)}}$ and $\boldsymbol{Y_{10}}^{M_p^{(5)}}$ equal.

B QEPs and QHPs in first- and second-order field-operator-moments spaces: Comparison

Here, we present tables that summarize the QEPs and QHPs, along with their degeneracies, as observed in the first- and second-order FOM spaces for the bosonic systems analyzed in the main text. This analysis follows the methodology developed in Ref. [43], which derives the genuine and induced QEPs and QHPs — together with their degeneracies — from the inherited QEPs and QHPs identified in the dynamics of first-order FOMs.

The genuine QEPs can be viewed as analogues of the inherited QEPs in the dynamical matrix of first-order FOMs, now extended to the dynamical matrices of higher-order FOMs. However, a crucial distinction arises due to the structure of higher-order FOMs, which are constructed as products of a fixed number of field operators, incorporating all combinations of annihilation and creation operators. These combinations include terms that are mutually related by commutation relations. Since such terms contribute to the system dynamics only once, only one representative term should be considered when analyzing spectral degeneracies — this yields the genuine QEPs.

In contrast, if all such terms are retained in the analysis, without accounting for redundancy due to commutation relations, the resulting degeneracies are referred to as induced QEPs. The same distinction applies to QHPs, leading to the identification of both genuine and induced QHPs [43]. Different configurations of QEPs and QHPs emerge across different models, highlighting the rich variety of spectral degeneracy structures and their implications for diverse physical phenomena.

For the two-mode bosonic system with its dynamical matrix $\boldsymbol{M}^{(2)}$ given in Eq. (3), we summarize the corresponding degeneracies up to second-order FOMs in Tab. 1. This provides a direct comparison of the QEP and QHP degeneracies observed in the dynamics

$\Lambda_j^{\mathbf{i}}$	$\Lambda_j^{\mathbf{r}}$	Moments		Moment deg.	Genuine and induced QHPs		Genuine QHPs	
					Partial QDP x QEP deg.	Partial QDP x QEP deg.	Partial QDP x QEP deg.	Partial QDP x QEP deg.
γ_+	$\mp\beta$	$\langle\hat{b}_1\rangle,\ \langle\hat{b}_1^\dagger\rangle$	$\langle\hat{\boldsymbol{B}}_1\rangle$	1	1x2	2x2	1x2	2x2
		$\langle\hat{b}_2\rangle,\ \langle\hat{b}_2^\dagger\rangle$	$\langle\hat{\boldsymbol{B}}_2\rangle$	1	1x2		1x2	
$2\gamma_+$	$\mp2\beta$	$\langle\hat{b}_1\hat{b}_2\rangle,\ \langle\hat{b}_1^\dagger\hat{b}_2^\dagger\rangle$	$\langle\hat{\boldsymbol{B}}_1\hat{\boldsymbol{B}}_2\rangle$	2	2x4	4x4	1x4	1x4 +
	$\beta-\beta$	$\langle\hat{b}_1^\dagger\hat{b}_2\rangle$		2				
	$\beta-\beta$	$\langle\hat{b}_1\hat{b}_2^\dagger\rangle$		2				
	$\mp2\beta$	$\langle\hat{b}_1^2\rangle,\ \langle\hat{b}_1^{\dagger2}\rangle$	$\langle\hat{\boldsymbol{B}}_1^2\rangle$	1	1x4		1x3	2x3
	$\beta-\beta$	$\langle\hat{b}_1^\dagger\hat{b}_1\rangle$		2				
	$\mp2\beta$	$\langle\hat{b}_2^2\rangle,\ \langle\hat{b}_2^{\dagger2}\rangle$	$\langle\hat{\boldsymbol{B}}_2^2\rangle$	1	1x4		1x3	
	$\beta-\beta$	$\langle\hat{b}_2^\dagger\hat{b}_2\rangle$		2				

Table 1: Real and imaginary parts of the complex eigenfrequencies $\Lambda_j^{\mathbf{r}} - i\Lambda_j^{\mathbf{i}}$ of the matrix $\boldsymbol{M}^{(2)}$ given in Eq. (3) for the two-mode bosonic system derived from the equations for the FOMs up to second order. The corresponding moments in the 'diagonalized' field operators are written together with their degeneracies (deg.) coming from different positions of the field operators. The DDs of QHPs (partial DDs) derived from the indicated FOMs and the EDs of the constituting QEPs are given. Both genuine and induced QEPs and QHPs are considered. The operator vectors $\hat{\boldsymbol{B}}_j$ for $j = 1,2$ are defined in the rows written for $\Lambda_j^{\mathbf{i}} = \gamma_+$ devoted to the first-order FOMs, i.e. $\hat{\boldsymbol{B}}_j \equiv [\hat{b}_j, \hat{b}_j^\dagger]$ for $j = 1,2$. Symbol $\hat{\boldsymbol{B}}_j\hat{\boldsymbol{B}}_k$, $j,k = 1,2$, stands for the tensorial product that provides four terms explicitly written in the rows for $\Lambda_j^{\mathbf{i}} = 2\gamma_+$; the terms derived from those explicitly written by using the commutation relations are omitted.

of first- and second-order FOMs. Notably, we identify genuine QEPs with a fourth-order ED in the second-order FOM dynamics, in contrast to the inherited QEPs exhibiting only second-order EDs in the first-order FOM dynamics.

It is instructive to compare the QEP and QHP degeneracies listed in Tab. 1 with those observed in systems featuring larger numbers of modes, as presented below. This comparison highlights how the spectral degeneracy structures in first-order FOMs evolve when extended to second-order FOMs. Notably, characteristic features emerge that can be generalized to spectral degeneracies of arbitrary-order FOMs, as discussed in Ref. [43]. For instance, one can infer the maximal EDs and maximal DDs occurring in the dynamics of FOMs of a given order.

Considering the linear three-mode bosonic system with its dynamical matrix $\boldsymbol{M}^{(3)}$ given in Eq. (21) under the condition given in Eq. (22), the QEPs and QHPs predicted in the dynamics of first- and second-order FOMs are summarized in Tab. 2. As shown there, the inherited QEPs with a third-order ED give rise to genuine QEPs with a ninth-order ED when analyzing the dynamics of second-order FOMs.

In the linear four-mode bosonic system described by the dynamical matrix $\boldsymbol{M}_1^{(4)}$ given in Eq. (28), which features equal damping and/or amplification rates for neighboring modes [see Eq. (29)], the QEPs and QHPs in the dynamics of first- and second-order FOMs are summarized in Tab. 3. These results also apply to the circular four-mode bosonic system with dynamical matrix $\boldsymbol{M}_{\mathrm{c}}^{(4)}$ shown in Eq. (38), assuming equal damping and/or amplification rates of neighboring modes [see Eq. (39). According to Tab. 3, the inherited

$\boldsymbol{\Lambda_j^i}$	$\boldsymbol{\Lambda_j^r}$	Moments		Moment deg.	Genuine and induced QHPs		Genuine QHPs	
					Partial QDP x QEP deg.	Partial QDP x QEP deg.	Partial QDP x QEP deg.	Partial QDP x QEP deg.
γ_+	$0, \mp\beta$	$\langle\hat{b}_1\rangle, \langle\hat{b}_2\rangle, \langle\hat{b}_2^\dagger\rangle$	$\langle\hat{\boldsymbol{B}}_1\rangle$	1	1x3	2x3	1x3	2x3
	$0, \mp\beta$	$\langle\hat{b}_1^\dagger\rangle, \langle\hat{b}_3\rangle, \langle\hat{b}_3^\dagger\rangle$	$\langle\hat{\boldsymbol{B}}_2\rangle$	1	1x3		1x3	
$2\gamma_+$	0	$\langle\hat{b}_1^2\rangle$	$\langle\hat{\boldsymbol{B}}_1^2\rangle$	1	1x9	4x9	1x6	2x6 +
	$\mp\beta$	$\langle\hat{b}_1\hat{b}_2\rangle, \langle\hat{b}_1\hat{b}_2^\dagger\rangle$		2				
	$\mp2\beta$	$\langle\hat{b}_2^2\rangle, \langle\hat{b}_2^{\dagger2}\rangle$		1				
	$\beta-\beta$	$\langle\hat{b}_2^\dagger\hat{b}_2\rangle$		2				
	0	$\langle\hat{b}_1^\dagger\hat{b}_1\rangle$	$\langle\hat{\boldsymbol{B}}_2\hat{\boldsymbol{B}}_1\rangle$	2	2x9		1x9	1x9
	$\mp\beta$	$\langle\hat{b}_1^\dagger\hat{b}_2\rangle, \langle\hat{b}_1^\dagger\hat{b}_2^\dagger\rangle$		2				
	$\mp\beta$	$\langle\hat{b}_3\hat{b}_1\rangle, \langle\hat{b}_3^\dagger\hat{b}_1\rangle$		2				
	$\mp2\beta$	$\langle\hat{b}_3\hat{b}_2\rangle, \langle\hat{b}_3^\dagger\hat{b}_2^\dagger\rangle$		2				
	$\beta-\beta$	$\langle\hat{b}_3\hat{b}_2^\dagger\rangle, \langle\hat{b}_3^\dagger\hat{b}_2\rangle$		2				
	0	$\langle\hat{b}_1^{\dagger2}\rangle$	$\langle\hat{\boldsymbol{B}}_2^2\rangle$	1	1x9		1x6	
	$\mp\beta$	$\langle\hat{b}_1^\dagger\hat{b}_3\rangle, \langle\hat{b}_1^\dagger\hat{b}_3^\dagger\rangle$		2				
	$\mp2\beta$	$\langle\hat{b}_3^2\rangle, \langle\hat{b}_3^{\dagger3}\rangle$		1				
	$\beta-\beta$	$\langle\hat{b}_3^\dagger\hat{b}_3\rangle$		2				

Table 2: Real and imaginary parts of the complex eigenfrequencies $\boldsymbol{\Lambda_j^r} - i\boldsymbol{\Lambda_j^i}$ of the matrix $\boldsymbol{M^{(3)}}$, given in Eq. (21), for the linear three-mode bosonic system derived from the equations for the FOMs up to second order. We have $\hat{\boldsymbol{B}}_1 \equiv [\hat{b}_1, \hat{b}_2, \hat{b}_2^\dagger]$ and $\hat{\boldsymbol{B}}_2 \equiv [\hat{b}_1^\dagger, \hat{b}_3, \hat{b}_3^\dagger]$ and more details are given in the caption to Tab. 1.

QEPs with doubled second-order ED give rise to genuine QEPs exhibiting fourth-order ED and sixth-order DD when analyzing second-order FOM dynamics.

On the other hand, for the linear four-mode bosonic system described by the dynamical matrix $\boldsymbol{M}_1^{(4)}$ given in Eq. (28), with varying damping and/or amplification rates of neighboring modes [see Eq. (33)], the QEPs and QHPs observed in the dynamics of first- and second-order FOMs are summarized in Tab. 4. The spectral structure of first-order FOMs, featuring two inherited QEPs with second-order EDs, evolves into a more complex second-order FOM structure that includes genuine QEPs with second-, third-, and fourth-order EDs. Notably, the genuine QHPs with second-order ED exhibit a sixteenth-order DD.

In the linear five-mode bosonic system described by the dynamical matrix $\boldsymbol{M}_1^{(5)}$ given in Eq. (44), with damping and/or amplification rates satisfying the conditions in Eqs. (45) and (46), the QEPs and QHPs observed in the dynamics of first- and second-order FOMs are summarized in Tab. 5. Notably, two inherited QEPs with second-order EDs give rise to genuine QEPs exhibiting second-, third-, and fourth-order EDs in various configurations within the spectral structure of second-order FOMs.

Finally, for the five-mode bosonic system in the pyramid configuration, described by the dynamical matrix $\boldsymbol{M}_p^{(5)}$ given in Eq. (51) with damping and/or amplification rates satisfying the conditions in Eqs. (52) and (53), the QEPs and QHPs identified in the dynamics of first- and second-order FOMs are systematically summarized in Tab. 6. Gen-

Λ_j^i	Λ_j^r	Moments		Moment deg.	Genuine and induced QHPs		Genuine QHPs	
					Partial QDP x QEP deg.	Partial QDP x QEP deg.	Partial QDP x QEP deg.	Partial QDP x QEP deg.
γ_+	$\alpha_\pm$	$\langle\hat{b}_1\rangle, \langle\hat{b}_3\rangle$	$\langle\hat{B}_1\rangle$	1	2x2	4x2	2x2	4x2
		$\langle\hat{b}_4\rangle, \langle\hat{b}_2\rangle$	$\langle\hat{B}_2\rangle$	1				
	$-\alpha_\pm$	$\langle\hat{b}_1^\dagger\rangle, \langle\hat{b}_3^\dagger\rangle$	$\langle\hat{B}_3\rangle$	1	2x2		2x2	
		$\langle\hat{b}_4^\dagger\rangle, \langle\hat{b}_2^\dagger\rangle$	$\langle\hat{B}_4\rangle$	1				
$2\gamma_+$	$2\alpha_\pm$	$\langle\hat{b}_1^2\rangle, \langle\hat{b}_3^2\rangle$	$\langle\hat{B}_1^2\rangle$	1	1x4	16x4	1x3	4x3 +
	$\alpha_-+\alpha_+$	$\langle\hat{b}_1\hat{b}_3\rangle$		2				
	$2\alpha_\mp$	$\langle\hat{b}_2^2\rangle, \langle\hat{b}_4^2\rangle$	$\langle\hat{B}_2^2\rangle$	1	1x4		1x3	
	$\alpha_-+\alpha_+$	$\langle\hat{b}_2\hat{b}_4\rangle$		2				
	$-2\alpha_\pm$	$\langle\hat{b}_1^{\dagger2}\rangle, \langle\hat{b}_3^{\dagger2}\rangle$	$\langle\hat{B}_3^2\rangle$	1	1x4		1x3	
	$-\alpha_--\alpha_+$	$\langle\hat{b}_1^\dagger\hat{b}_3^\dagger\rangle$		2				
	$-2\alpha_\mp$	$\langle\hat{b}_2^{\dagger2}\rangle, \langle\hat{b}_4^{\dagger2}\rangle$	$\langle\hat{B}_4^2\rangle$	1	1x4		1x3	
	$-\alpha_--\alpha_+$	$\langle\hat{b}_2^\dagger\hat{b}_4^\dagger\rangle$		2				
	$-\alpha_\pm+\alpha_\pm$	$\langle\hat{b}_1^\dagger\hat{b}_1\rangle, \langle\hat{b}_3^\dagger\hat{b}_3\rangle$	$\langle\hat{B}_3\hat{B}_1\rangle$	2	2x4		1x4	6x4
	$\pm\alpha_-\mp\alpha_+$	$\langle\hat{b}_1^\dagger\hat{b}_3\rangle, \langle\hat{b}_1\hat{b}_3^\dagger\rangle$		2				
	$-\alpha_\mp+\alpha_\mp$	$\langle\hat{b}_2^\dagger\hat{b}_2\rangle, \langle\hat{b}_4^\dagger\hat{b}_4\rangle$	$\langle\hat{B}_4\hat{B}_2\rangle$	2	2x4		1x4	
	$\mp\alpha_-\pm\alpha_+$	$\langle\hat{b}_2^\dagger\hat{b}_4\rangle, \langle\hat{b}_4^\dagger\hat{b}_2\rangle$		2				
	$\alpha_++\alpha_-$	$\langle\hat{b}_1\hat{b}_2\rangle, \langle\hat{b}_3\hat{b}_4\rangle$	$\langle\hat{B}_1\hat{B}_2\rangle$	2	2x4		1x4	
	$2\alpha_\pm$	$\langle\hat{b}_1\hat{b}_4\rangle, \langle\hat{b}_3\hat{b}_2\rangle$		2				
	$\alpha_\mp-\alpha_\pm$	$\langle\hat{b}_1^\dagger\hat{b}_2\rangle, \langle\hat{b}_3^\dagger\hat{b}_4\rangle$	$\langle\hat{B}_3\hat{B}_2\rangle$	2	2x4		1x4	
	$\alpha_\pm-\alpha_\pm$	$\langle\hat{b}_1^\dagger\hat{b}_4\rangle, \langle\hat{b}_3^\dagger\hat{b}_2\rangle$		2				
	$\alpha_\pm-\alpha_\mp$	$\langle\hat{b}_2^\dagger\hat{b}_1\rangle, \langle\hat{b}_4^\dagger\hat{b}_3\rangle$	$\langle\hat{B}_4\hat{B}_1\rangle$	2	2x4		1x4	
	$\alpha_\pm-\alpha_\pm$	$\langle\hat{b}_4^\dagger\hat{b}_1\rangle, \langle\hat{b}_2^\dagger\hat{b}_3\rangle$		2				
	$-\alpha_+-\alpha_-$	$\langle\hat{b}_1^\dagger\hat{b}_2^\dagger\rangle, \langle\hat{b}_3^\dagger\hat{b}_4^\dagger\rangle$	$\langle\hat{B}_3\hat{B}_4\rangle$	2	2x4		1x4	
	$-2\alpha_\pm$	$\langle\hat{b}_1^\dagger\hat{b}_4^\dagger\rangle, \langle\hat{b}_3^\dagger\hat{b}_2^\dagger\rangle$		2				

Table 3: Real and imaginary parts of the complex eigenfrequencies $\Lambda_j^r - i\Lambda_j^i$ of the matrix $M_{11}^{(4)}$, given in Eq. (28) with Eq. (29), for the linear four-mode bosonic system with equal damping and/or amplification rates for neighbor modes derived from the equations for the FOMs up to second order. We note that $\alpha_\pm(\zeta) = \alpha_\mp(-\zeta)$ is used here. We have $\hat{B}_1 \equiv [\hat{b}_1, \hat{b}_3]$, $\hat{B}_2 \equiv [\hat{b}_2, \hat{b}_4]$, $\hat{B}_3 = \hat{B}_1^\dagger$, $\hat{B}_4 = \hat{B}_2^\dagger$. More details are given in the caption to Tab. 1.

$\mathbf{\Lambda_j^i}$	$\mathbf{\Lambda_j^r}$	Moments		Moment deg.	Genuine and induced QHPs		Genuine QHPs	
					Partial QDP x QEP deg.	Partial QDP x QEP deg.	Partial QDP x QEP deg.	Partial QDP x QEP deg.
γ_+	$\pm\alpha_+$	$\langle\hat{b}_1\rangle, \langle\hat{b}_1^\dagger\rangle$	$\langle\hat{\boldsymbol{B}}_1\rangle$	1	1x2	2x2	1x2	2x2
		$\langle\hat{b}_2\rangle, \langle\hat{b}_2^\dagger\rangle$	$\langle\hat{\boldsymbol{B}}_2\rangle$	1	1x2		1x2	
	α_-	$\langle\hat{b}_3\rangle$	$\langle\hat{\boldsymbol{B}}_3\rangle$	1	2x1	2x1	2x1	2x1
		$\langle\hat{b}_4\rangle$	$\langle\hat{\boldsymbol{B}}_4\rangle$	1				
	$-\alpha_-$	$\langle\hat{b}_3^\dagger\rangle$	$\langle\hat{\boldsymbol{B}}_5\rangle$	1	2x1	2x1	2x1	2x1
		$\langle\hat{b}_4^\dagger\rangle$	$\langle\hat{\boldsymbol{B}}_6\rangle$	1				
$2\gamma_+$	$\pm2\alpha_+$ $\alpha_+-\alpha_+$	$\langle\hat{b}_1^2\rangle, \langle\hat{b}_1^{\dagger2}\rangle$ $\langle\hat{b}_1^\dagger\hat{b}_1\rangle$	$\langle\hat{\boldsymbol{B}}_1^2\rangle$	1 2	1x4	4x4	1x3	2x3 +
	$\pm2\alpha_+$ $\alpha_+-\alpha_+$	$\langle\hat{b}_2^2\rangle, \langle\hat{b}_2^{\dagger2}\rangle$ $\langle\hat{b}_2^\dagger\hat{b}_2\rangle$	$\langle\hat{\boldsymbol{B}}_2^2\rangle$	1 2	1x4		1x3	
	$\pm\alpha_+$ $\alpha_+-\alpha_+$	$\langle\hat{b}_1\hat{b}_2\rangle, \langle\hat{b}_1^\dagger\hat{b}_2\rangle$ $\langle\hat{b}_1^\dagger\hat{b}_2\rangle, \langle\hat{b}_1\hat{b}_2^\dagger\rangle$	$\langle\hat{\boldsymbol{B}}_1\hat{\boldsymbol{B}}_2\rangle$	2 2	2x4		1x4	1x4
	$\alpha_-\pm\alpha_+$	$\langle\hat{b}_1\hat{b}_3\rangle, \langle\hat{b}_1^\dagger\hat{b}_3\rangle$	$\langle\hat{\boldsymbol{B}}_1\hat{\boldsymbol{B}}_3\rangle$	2	2x2	16x2	2x2	16x2
		$\langle\hat{b}_1\hat{b}_4\rangle, \langle\hat{b}_1^\dagger\hat{b}_4\rangle$	$\langle\hat{\boldsymbol{B}}_1\hat{\boldsymbol{B}}_4\rangle$	2	2x2		2x2	
	$\alpha_-\pm\alpha_+$	$\langle\hat{b}_2\hat{b}_3\rangle, \langle\hat{b}_2^\dagger\hat{b}_3\rangle$	$\langle\hat{\boldsymbol{B}}_2\hat{\boldsymbol{B}}_3\rangle$	2	2x2		2x2	
		$\langle\hat{b}_2\hat{b}_4\rangle, \langle\hat{b}_2^\dagger\hat{b}_4\rangle$	$\langle\hat{\boldsymbol{B}}_2\hat{\boldsymbol{B}}_4\rangle$	2	2x2		2x2	
	$-\alpha_-\pm\alpha_+$	$\langle\hat{b}_1\hat{b}_3^\dagger\rangle, \langle\hat{b}_1^\dagger\hat{b}_3^\dagger\rangle$	$\langle\hat{\boldsymbol{B}}_1\hat{\boldsymbol{B}}_5\rangle$	2	2x2		2x2	
		$\langle\hat{b}_1\hat{b}_4^\dagger\rangle, \langle\hat{b}_1^\dagger\hat{b}_4^\dagger\rangle$	$\langle\hat{\boldsymbol{B}}_1\hat{\boldsymbol{B}}_6\rangle$	2	2x2		2x2	
	$-\alpha_-\pm\alpha_+$	$\langle\hat{b}_2\hat{b}_3^\dagger\rangle, \langle\hat{b}_2^\dagger\hat{b}_3^\dagger\rangle$	$\langle\hat{\boldsymbol{B}}_2\hat{\boldsymbol{B}}_5\rangle$	2	2x2		2x2	
		$\langle\hat{b}_2\hat{b}_4^\dagger\rangle, \langle\hat{b}_2^\dagger\hat{b}_4^\dagger\rangle$	$\langle\hat{\boldsymbol{B}}_2\hat{\boldsymbol{B}}_6\rangle$	2	2x2		2x2	
	$2\alpha_-$	$\langle\hat{b}_3^2\rangle, \langle\hat{b}_4^2\rangle$	$\langle\hat{\boldsymbol{B}}_3^2\rangle,$ $\langle\hat{\boldsymbol{B}}_4^2\rangle$	1	4x1	4x1	3x1	3x1
		$\langle\hat{b}_3\hat{b}_4\rangle$	$\langle\hat{\boldsymbol{B}}_3\hat{\boldsymbol{B}}_4\rangle$	2				
	$-2\alpha_-$	$\langle\hat{b}_3^{\dagger2}\rangle, \langle\hat{b}_4^{\dagger2}\rangle$	$\langle\hat{\boldsymbol{B}}_5^2\rangle,$ $\langle\hat{\boldsymbol{B}}_6^2\rangle$	1	4x1	4x1	3x1	3x1
		$\langle\hat{b}_3^\dagger\hat{b}_4^\dagger\rangle$	$\langle\hat{\boldsymbol{B}}_5\hat{\boldsymbol{B}}_6\rangle$	2				
	$\alpha_--\alpha_-$	$\langle\hat{b}_3^\dagger\hat{b}_3\rangle, \langle\hat{b}_4^\dagger\hat{b}_4\rangle$	$\langle\hat{\boldsymbol{B}}_5\hat{\boldsymbol{B}}_3\rangle,$ $\langle\hat{\boldsymbol{B}}_6\hat{\boldsymbol{B}}_4\rangle$	2	8x1	8x1	4x1	4x1
		$\langle\hat{b}_3^\dagger\hat{b}_4\rangle, \langle\hat{b}_3\hat{b}_4^\dagger\rangle$	$\langle\hat{\boldsymbol{B}}_5\hat{\boldsymbol{B}}_4\rangle,$ $\langle\hat{\boldsymbol{B}}_3\hat{\boldsymbol{B}}_6\rangle$	2				

Table 4: Real and imaginary parts of the complex eigenfrequencies $\mathbf{\Lambda_j^r} - i\mathbf{\Lambda_j^i}$ of the matrix $M_{12}^{(4)}$, given in Eq. (28) with Eq. (33) for the linear four-mode bosonic system with different damping and/or amplification rates of neighbor modes, as derived from the equations for the FOMs up to second order assuming $\alpha_+ = 0$. We have $\hat{\boldsymbol{B}}_j \equiv [\hat{b}_j, \hat{b}_j^\dagger]$ for $j = 1, 2$, $\hat{\boldsymbol{B}}_j \equiv [\hat{b}_j]$ for $j = 3, 4$, $\hat{\boldsymbol{B}}_5 = \hat{\boldsymbol{B}}_3^\dagger$, $\hat{\boldsymbol{B}}_6 = \hat{\boldsymbol{B}}_4^\dagger$ and more details are given in the caption to Tab. 1.

Λ_j^i	Λ_j^r	Moments		Moment deg.	Genuine and induced QHPs		Genuine QHPs	
					Partial QDP x QEP deg.	Partial QDP x QEP deg.	Partial QDP x QEP deg.	Partial QDP x QEP deg.
γ_+	$\alpha_\mp$	$\langle \hat{b}_2\rangle, \langle \hat{b}_4\rangle$	$\langle \hat{B}_1\rangle$	1	2x2	4x2	2x2	4x2
		$\langle \hat{b}_3\rangle, \langle \hat{b}_5\rangle$	$\langle \hat{B}_2\rangle$	1				
	$-\alpha_\mp$	$\langle \hat{b}_2^\dagger\rangle, \langle \hat{b}_4^\dagger\rangle$	$\langle \hat{B}_3\rangle$	1	2x2		2x2	
		$\langle \hat{b}_3^\dagger\rangle, \langle \hat{b}_5^\dagger\rangle$	$\langle \hat{B}_4\rangle$	1				
	0	$\langle \hat{b}_1\rangle$	$\langle \hat{B}_5\rangle$	1	2x1	2x1	2x1	2x1
		$\langle \hat{b}_1^\dagger\rangle$	$\langle \hat{B}_6\rangle$	1				
$2\gamma_+$	$2\alpha_\mp$	$\langle \hat{b}_2^2\rangle, \langle \hat{b}_4^2\rangle$	$\langle \hat{B}_1^2\rangle$	1	1x4	16x4	1x3	4x3 +
	$\alpha_- + \alpha_+$	$\langle \hat{b}_2\hat{b}_4\rangle$		2				
	$2\alpha_\mp$	$\langle \hat{b}_3^2\rangle, \langle \hat{b}_5^2\rangle$	$\langle \hat{B}_2^2\rangle$	1	1x4		1x3	
	$\alpha_- + \alpha_+$	$\langle \hat{b}_3\hat{b}_5\rangle$		2				
	$-2\alpha_\mp$	$\langle \hat{b}_2^{\dagger 2}\rangle, \langle \hat{b}_4^{\dagger 2}\rangle$	$\langle \hat{B}_3^2\rangle$	1	1x4		1x3	
	$-\alpha_- - \alpha_+$	$\langle \hat{b}_2^\dagger \hat{b}_4^\dagger\rangle$		2				
	$-2\alpha_\mp$	$\langle \hat{b}_3^{\dagger 2}\rangle, \langle \hat{b}_5^{\dagger 2}\rangle$	$\langle \hat{B}_4^2\rangle$	1	1x4		1x3	
	$-\alpha_- - \alpha_+$	$\langle \hat{b}_3^\dagger \hat{b}_5^\dagger\rangle$		2				
	$2\alpha_\mp$	$\langle \hat{b}_2\hat{b}_3\rangle, \langle \hat{b}_4\hat{b}_5\rangle$	$\langle \hat{B}_1\hat{B}_2\rangle$	2	2x4		1x4	
	$\alpha_+ + \alpha_-$	$\langle \hat{b}_2\hat{b}_5\rangle, \langle \hat{b}_4\hat{b}_3\rangle$		2				
	$-\alpha_\mp + \alpha_\mp$	$\langle \hat{b}_2^\dagger \hat{b}_2\rangle, \langle \hat{b}_4^\dagger \hat{b}_4\rangle$	$\langle \hat{B}_3\hat{B}_1\rangle$	2	2x4		1x4	
	$-\alpha_\mp + \alpha_\pm$	$\langle \hat{b}_2^\dagger \hat{b}_4\rangle, \langle \hat{b}_2\hat{b}_4^\dagger\rangle$		2				
	$\alpha_\mp - \alpha_\mp$	$\langle \hat{b}_3^\dagger \hat{b}_2\rangle, \langle \hat{b}_5^\dagger \hat{b}_4\rangle$	$\langle \hat{B}_4\hat{B}_1\rangle$	2	2x4		1x4	6x4
	$\alpha_\pm - \alpha_\mp$	$\langle \hat{b}_5^\dagger \hat{b}_2\rangle, \langle \hat{b}_3^\dagger \hat{b}_4\rangle$		2				
	$\alpha_\mp - \alpha_\mp$	$\langle \hat{b}_2^\dagger \hat{b}_3\rangle, \langle \hat{b}_4^\dagger \hat{b}_5\rangle$	$\langle \hat{B}_3\hat{B}_2\rangle$	2	2x4		1x4	
	$\alpha_\pm - \alpha_\mp$	$\langle \hat{b}_2^\dagger \hat{b}_5\rangle, \langle \hat{b}_4^\dagger \hat{b}_3\rangle$		2				
	$-\alpha_\mp + \alpha_\mp$	$\langle \hat{b}_3^\dagger \hat{b}_3\rangle, \langle \hat{b}_5^\dagger \hat{b}_5\rangle$	$\langle \hat{B}_4\hat{B}_2\rangle$	2	2x4		1x4	
	$-\alpha_\mp + \alpha_\pm$	$\langle \hat{b}_3^\dagger \hat{b}_5\rangle, \langle \hat{b}_5^\dagger \hat{b}_3\rangle$		2				
	$-2\alpha_\mp$	$\langle \hat{b}_2^\dagger \hat{b}_3^\dagger\rangle, \langle \hat{b}_4^\dagger \hat{b}_5^\dagger\rangle$	$\langle \hat{B}_3\hat{B}_4\rangle$	2	2x4		1x4	
	$-\alpha_+ - \alpha_-$	$\langle \hat{b}_2^\dagger \hat{b}_5^\dagger\rangle, \langle \hat{b}_4^\dagger \hat{b}_3^\dagger\rangle$		2				
	$\alpha_\mp$	$\langle \hat{b}_2\hat{b}_1\rangle, \langle \hat{b}_4\hat{b}_1\rangle$	$\langle \hat{B}_1\hat{B}_5\rangle$	2	8x2	16x2	4x2	8x2
		$\langle \hat{b}_2\hat{b}_1^\dagger\rangle \langle \hat{b}_4\hat{b}_1^\dagger\rangle$	$\langle \hat{B}_1\hat{B}_6\rangle$	2				
		$\langle \hat{b}_3\hat{b}_1\rangle, \langle \hat{b}_5\hat{b}_1\rangle$	$\langle \hat{B}_2\hat{B}_5\rangle$	2				
		$\langle \hat{b}_3\hat{b}_1^\dagger\rangle \langle \hat{b}_5\hat{b}_1^\dagger\rangle$	$\langle \hat{B}_2\hat{B}_6\rangle$	2				
	$-\alpha_\mp$	$\langle \hat{b}_2^\dagger \hat{b}_1\rangle, \langle \hat{b}_4^\dagger \hat{b}_1\rangle$	$\langle \hat{B}_3\hat{B}_5\rangle$	2	8x2		4x2	
		$\langle \hat{b}_2^\dagger \hat{b}_1^\dagger\rangle \langle \hat{b}_4^\dagger \hat{b}_1^\dagger\rangle$	$\langle \hat{B}_3\hat{B}_6\rangle$	2				
		$\langle \hat{b}_3^\dagger \hat{b}_1\rangle, \langle \hat{b}_5^\dagger \hat{b}_1\rangle$	$\langle \hat{B}_4\hat{B}_5\rangle$	2				
		$\langle \hat{b}_3^\dagger \hat{b}_1^\dagger\rangle \langle \hat{b}_5^\dagger \hat{b}_1^\dagger\rangle$	$\langle \hat{B}_4\hat{B}_6\rangle$	2				
	0	$\langle \hat{b}_1^2\rangle, \langle \hat{b}_1^{\dagger 2}\rangle$	$\langle \hat{B}_5^2\rangle, \langle \hat{B}_6^2\rangle$	1	4x1	4x1	3x1	3x1
		$\langle \hat{b}_1^\dagger \hat{b}_1\rangle$	$\langle \hat{B}_6\hat{B}_5\rangle$	2				

Table 5: Real and imaginary parts of the complex eigenfrequencies $\Lambda_j^r - i\Lambda_j^i$ of the matrix $M_1^{(5)}$, given in Eq. (44), for the five-mode linear bosonic system derived from the equations for the FOMs up to second order. We have $\hat{B}_1 \equiv [\hat{b}_2, \hat{b}_4]$, $\hat{B}_2 \equiv [\hat{b}_3, \hat{b}_5]$, $\hat{B}_3 = \hat{B}_1^\dagger$, $\hat{B}_4 = \hat{B}_2^\dagger$, $\hat{B}_5 \equiv [\hat{b}_1]$, $\hat{B}_6 = \hat{B}_5^\dagger$, and more details are given in the caption to Tab. 1.

$\mathbf{\Lambda_j^i}$	$\mathbf{\Lambda_j^r}$	Moments		Moment deg.	Genuine and induced QHPs		Genuine QHPs	
					Partial QDP x QEP deg.	Partial QDP x QEP deg.	Partial QDP x QEP deg.	Partial QDP x QEP deg.
γ_+	$-\zeta \mp \beta_2$	$\langle \hat{b}_4 \rangle, \langle \hat{b}_5^\dagger \rangle$	$\langle \hat{B}_1 \rangle$	1	1x2	1x2	1x2	1x2
	$\zeta \pm \beta_2$	$\langle \hat{b}_4^\dagger \rangle, \langle \hat{b}_5 \rangle$	$\langle \hat{B}_2 \rangle$	1	1x2	1x2	1x2	1x2
	$\zeta - \beta_1$	$\langle \hat{b}_2 \rangle$	$\langle \hat{B}_3 \rangle$	1	1x1	1x1	1x1	1x1
	$-\zeta + \beta_1$	$\langle \hat{b}_2^\dagger \rangle$	$\langle \hat{B}_4 \rangle$	1	1x1	1x1	1x1	1x1
	$-\zeta - \beta_1$	$\langle \hat{b}_3 \rangle$	$\langle \hat{B}_5 \rangle$	1	1x1	1x1	1x1	1x1
	$\zeta + \beta_1$	$\langle \hat{b}_3^\dagger \rangle$	$\langle \hat{B}_6 \rangle$	1	1x1	1x1	1x1	1x1
	0	$\langle \hat{b}_1 \rangle$	$\langle \hat{B}_7 \rangle$	1	2x1	2x1	2x1	2x1
		$\langle \hat{b}_1^\dagger \rangle$	$\langle \hat{B}_8 \rangle$	1				
$2\gamma_+$	$-2\zeta \mp 2\beta_2$	$\langle \hat{b}_4^2 \rangle, \langle \hat{b}_5^{\dagger 2} \rangle$	$\langle \hat{B}_1^2 \rangle$	1	1x4	1x4	1x3	1x3
	-2ζ	$\langle \hat{b}_5^\dagger \hat{b}_4 \rangle$		2				
	$2\zeta \pm 2\beta_2$	$\langle \hat{b}_4^{\dagger 2} \rangle, \langle \hat{b}_5^2 \rangle$	$\langle \hat{B}_2^2 \rangle$	1	1x4	1x4	1x3	1x3
	2ζ	$\langle \hat{b}_4^\dagger \hat{b}_5 \rangle$		2				
	$2\zeta - 2\beta_1$	$\langle \hat{b}_2^2 \rangle$	$\langle \hat{B}_3^2 \rangle$	1	1x1	1x1	1x1	1x1
	$-2\zeta + 2\beta_1$	$\langle \hat{b}_2^{\dagger 2} \rangle$	$\langle \hat{B}_4^2 \rangle$	1	1x1	1x1	1x1	1x1
	$-2\zeta - 2\beta_1$	$\langle \hat{b}_3^2 \rangle$	$\langle \hat{B}_5^2 \rangle$	1	1x1	1x1	1x1	1x1
	$2\zeta + 2\beta_1$	$\langle \hat{b}_3^{\dagger 2} \rangle$	$\langle \hat{B}_6^2 \rangle$	1	1x1	1x1	1x1	1x1
	0	$\langle \hat{b}_1^2 \rangle, \langle \hat{b}_1^{\dagger 2} \rangle$	$\langle \hat{B}_7^2 \rangle, \langle \hat{B}_8^2 \rangle$	1	4x1	4x1	3x1	3x1
		$\langle \hat{b}_1^\dagger \hat{b}_1 \rangle$	$\langle \hat{B}_8 \hat{B}_7 \rangle$	2				
	$\pm 2\beta_2$	$\langle \hat{b}_4^\dagger \hat{b}_5^\dagger \rangle, \langle \hat{b}_4 \hat{b}_5 \rangle$	$\langle \hat{B}_2 \hat{B}_1 \rangle$	2	2x4	2x4	1x4	1x4
	$\beta_2 - \beta_2$	$\langle \hat{b}_4^\dagger \hat{b}_4 \rangle, \langle \hat{b}_5 \hat{b}_5^\dagger \rangle$		2				
	$-\beta_1 \mp \beta_2$	$\langle \hat{b}_4 \hat{b}_2 \rangle, \langle \hat{b}_5^\dagger \hat{b}_2 \rangle$	$\langle \hat{B}_1 \hat{B}_3 \rangle$	2	4x1	4x1	2x1	2x1
	$2\zeta - \beta_1 \pm \beta_2$	$\langle \hat{b}_4^\dagger \hat{b}_2 \rangle, \langle \hat{b}_5 \hat{b}_2 \rangle$	$\langle \hat{B}_2 \hat{B}_3 \rangle$	2	4x1	4x1	2x1	2x1
	$-2\zeta + \beta_1 \mp \beta_2$	$\langle \hat{b}_2^\dagger \hat{b}_4 \rangle, \langle \hat{b}_2^\dagger \hat{b}_5^\dagger \rangle$	$\langle \hat{B}_4 \hat{B}_1 \rangle$	2	4x1	4x1	2x1	2x1
	$\beta_1 \pm \beta_2$	$\langle \hat{b}_2^\dagger \hat{b}_4^\dagger \rangle, \langle \hat{b}_2^\dagger \hat{b}_5 \rangle$	$\langle \hat{B}_4 \hat{B}_2 \rangle$	2	4x1	4x1	2x1	2x1
	$-2\zeta - \beta_1 \mp \beta_2$	$\langle \hat{b}_4 \hat{b}_3 \rangle, \langle \hat{b}_5^\dagger \hat{b}_3 \rangle$	$\langle \hat{B}_1 \hat{B}_5 \rangle$	2	4x1	4x1	2x1	2x1
	$-\beta_1 \pm \beta_2$	$\langle \hat{b}_4^\dagger \hat{b}_3 \rangle, \langle \hat{b}_5 \hat{b}_3 \rangle$	$\langle \hat{B}_2 \hat{B}_5 \rangle$	2	4x1	4x1	2x1	2x1
	$\beta_1 \mp \beta_2$	$\langle \hat{b}_3^\dagger \hat{b}_4 \rangle, \langle \hat{b}_3^\dagger \hat{b}_5^\dagger \rangle$	$\langle \hat{B}_6 \hat{B}_1 \rangle$	2	4x1	4x1	2x1	2x1
	$2\zeta + \beta_1 \pm \beta_2$	$\langle \hat{b}_3^\dagger \hat{b}_4^\dagger \rangle, \langle \hat{b}_3^\dagger \hat{b}_5 \rangle$	$\langle \hat{B}_6 \hat{B}_2 \rangle$	2	4x1	4x1	2x1	2x1
	$-\zeta \mp \beta_2$	$\langle \hat{b}_4 \hat{b}_1 \rangle, \langle \hat{b}_5^\dagger \hat{b}_1 \rangle$	$\langle \hat{B}_7 \hat{B}_1 \rangle$	2	4x2	4x2	2x2	2x2
		$\langle \hat{b}_4 \hat{b}_1^\dagger \rangle, \langle \hat{b}_5^\dagger \hat{b}_1^\dagger \rangle$	$\langle \hat{B}_8 \hat{B}_1 \rangle$	2				
	$\zeta \pm \beta_2$	$\langle \hat{b}_4^\dagger \hat{b}_1 \rangle, \langle \hat{b}_5 \hat{b}_1 \rangle$	$\langle \hat{B}_7 \hat{B}_2 \rangle$	2	4x2	4x2	2x2	2x2
		$\langle \hat{b}_4^\dagger \hat{b}_1^\dagger \rangle, \langle \hat{b}_5 \hat{b}_1^\dagger \rangle$	$\langle \hat{B}_8 \hat{B}_2 \rangle$	2				
	$\beta_1 - \beta_1$	$\langle \hat{b}_2^\dagger \hat{b}_2 \rangle$	$\langle \hat{B}_4 \hat{B}_3 \rangle$	2	2x1	2x1	1x1	1x1
	$-2\beta_1$	$\langle \hat{b}_3 \hat{b}_2 \rangle$	$\langle \hat{B}_5 \hat{B}_3 \rangle$	2	2x1	2x1	1x1	1x1
	2ζ	$\langle \hat{b}_3^\dagger \hat{b}_2 \rangle$	$\langle \hat{B}_6 \hat{B}_3 \rangle$	2	2x1	2x1	1x1	1x1
	$\zeta - \beta_1$	$\langle \hat{b}_1 \hat{b}_2 \rangle$	$\langle \hat{B}_7 \hat{B}_3 \rangle$	2	4x1	4x1	2x1	2x1
		$\langle \hat{b}_1^\dagger \hat{b}_2 \rangle$	$\langle \hat{B}_8 \hat{B}_3 \rangle$	2				
	-2ζ	$\langle \hat{b}_2^\dagger \hat{b}_3 \rangle$	$\langle \hat{B}_4 \hat{B}_5 \rangle$	2	2x1	2x1	1x1	1x1
	$2\beta_1$	$\langle \hat{b}_2^\dagger \hat{b}_3^\dagger \rangle$	$\langle \hat{B}_4 \hat{B}_6 \rangle$	2	2x1	2x1	1x1	1x1
	$-\zeta - \beta_1$	$\langle \hat{b}_2^\dagger \hat{b}_1 \rangle$	$\langle \hat{B}_4 \hat{B}_7 \rangle$	2	4x1	4x1	2x1	2x1
		$\langle \hat{b}_2^\dagger \hat{b}_1^\dagger \rangle$	$\langle \hat{B}_4 \hat{B}_8 \rangle$	2				
	$\beta_1 - \beta_1$	$\langle \hat{b}_3^\dagger \hat{b}_3 \rangle$	$\langle \hat{B}_6 \hat{B}_5 \rangle$	2	2x1	2x1	1x1	1x1
	$-\zeta - \beta_1$	$\langle \hat{b}_1 \hat{b}_3 \rangle$	$\langle \hat{B}_7 \hat{B}_5 \rangle$	2	4x1	4x1	2x1	2x1
		$\langle \hat{b}_1^\dagger \hat{b}_3 \rangle$	$\langle \hat{B}_8 \hat{B}_5 \rangle$	2				
	$\zeta + \beta_1$	$\langle \hat{b}_3^\dagger \hat{b}_1 \rangle$	$\langle \hat{B}_6 \hat{B}_7 \rangle$	2	4x1	4x1	2x1	2x1
		$\langle \hat{b}_3^\dagger \hat{b}_1^\dagger \rangle$	$\langle \hat{B}_6 \hat{B}_8 \rangle$	2				

Table 6: Real and imaginary parts of the complex eigenfrequencies $\Lambda_j^r - i\Lambda_j^i$ of the matrix $M_p^{(5)}$, given in Eq. (51), for the five-mode pyramid bosonic system derived from the equations for the FOMs up to second order assuming $\beta_2 = 0$. If $\beta_1 = 0$ instead of $\beta_2 = 0$, simple relabelling of $\hat{b}_j$, $\hat{b}_j^\dagger$ operators provides the corresponding table. We have $\hat{B}_1 \equiv [\hat{b}_4, \hat{b}_5^\dagger]$, $\hat{B}_2 = \hat{B}_1^\dagger$, $\hat{B}_3 \equiv [\hat{b}_2]$, $\hat{B}_4 = \hat{B}_3^\dagger$, $\hat{B}_5 \equiv [\hat{b}_3]$, $\hat{B}_6 = \hat{B}_5^\dagger$, $\hat{B}_7 \equiv [\hat{b}_1]$, $\hat{B}_8 = \hat{B}_7^\dagger$, and more details are given in the caption to Tab. 1.

uine QEPs with second-, third-, and fourth-order EDs appear in the spectral structure of second-order FOMs, though with relatively low DDs. This reflects the limited presence of DDs in the first-order FOM spectra, where only one eigenfrequency exhibits a second-order DD.

References

[1] C. M. Bender and S. Boettcher. "Real spectra in non-Hermitian Hamiltonians having $\mathcal{PT}$ symmetry". Phys. Rev. Lett. **80**, 5243–5246 (1998).

[2] C. M. Bender, D. C. Brody, and H. F. Jones. "Must a Hamiltonian be Hermitian?". Am. J. Phys. **71**, 1095–1102 (2003).

[3] C. M. Bender. "Making sense of non-Hermitian Hamiltonians". Contemp. Phys. **70**, 947 (2007).

[4] R. El-Ganainy, K. G. Makris, M. Khajavikhan, Z. H. Musslimani, S. Rotter, and D. N. Christodoulides. "Non-Hermitian physics and $\mathcal{PT}$ symmetry". Nat. Phys. **14**, 11 (2018).

[5] Y. Ashida, Z. Gong, and M. Ueda. "Non-Hermitian physics". Adv. Phys. **69**, 249 (2020).

[6] A. Mostafazadeh. "Pseudo-Hermiticity and generalized $\mathcal{PT}$ and $\mathcal{CPT}$-symmetries". J. Math. Phys. (Melville, NY) **44**, 974 (2003).

[7] A. Mostafazadeh. "Time dependent Hilbert spaces, geometric phases, and general covariance in quantum mechanics". Phys. Lett. A **320**, 375 (2004).

[8] A. Mostafazadeh. "Pseudo-Hermitian representation of quantum mechanics". Int. J. Geom. Meth. Mod. Phys. **7**, 1191 (2010).

[9] M. Znojil. "Time-dependent version of crypto-Hermitian quantum theory". Phys. Rev. D **78**, 085003 (2008).

[10] D. C. Brody. "Biorthogonal quantum mechanics". J. Phys. A: Math. Theor. **47**, 035305 (2014).

[11] F. Bagarello, R. Passante, and C. Trapani. "Non-Hermitian Hamiltonians in quantum physics". Volume 184. Springer, New York. (2016).

[12] W. Chen, Ş. Kaya Özdemir, G. Zhao, J. Wiersig, and L. Yang. "Exceptional points enhance sensing in an optical microcavity". Nature (London) **548**, 192–196 (2017).

[13] Z.-P. Liu, J. Zhang, Ş. K. Özdemir, B. Peng, H. Jing, X.-Y. Lü, C.-W. Li, L. Yang, F. Nori, and Y.-X. Liu. "Metrology with $\mathcal{PT}$-symmetric cavities: Enhanced sensitivity near the $\mathcal{PT}$-phase transition". Phys. Rev. Lett. **117**, 110802 (2016).

[14] L. Feng, R. El-Ganainy, and L. Ge. "Non-Hermitian photonics based on parity–time symmetry". Nat. Photon. **11**, 752 (2017).

[15] R. El-Ganainy, M. Khajavikhan, S. Rotter, D. N. Christodoulides, and Ş. K. Özdemir. "The dawn of Non-Hermitian optics". Commun. Phys. **2**, 37 (2019).

[16] M. Parto, Y. G. N. Liu, B. Bahari, M. Khajavikhan, and D. N. Christodoulides. "Non-Hermitian and topological photonics: Optics at an exceptional point". Nanophotonics **10**, 403 (2021).

[17] J. Peřina Jr. and A. Lukš. "Quantum behavior of a $\mathcal{PT}$-symmetric two-mode system with cross-Kerr nonlinearity". Symmetry **11**, 1020 (2019).

[18] J. Peřina Jr., A. Lukš, J. K. Kalaga, W. Leoński, and A. Miranowicz. "Nonclassical light at exceptional points of a quantum $\mathcal{PT}$-symmetric two-mode system". Phys. Rev. A **100**, 053820 (2019).

[19] E. G. Turitsyna, I. V. Shadrivov, and Y. S. Kivshar. "Guided modes in non-Hermitian optical waveguides". Phys. Rev. A **96**, 033824 (2017).

[20] X. Xu, L. Shi, L. Ren, and X. Zhang. "Optical gradient forces in $\mathcal{PT}$-symmetric coupled-waveguide structures". Opt. Express **26**, 10220–10229 (2018).

[21] E.-M. Graefe and H. F. Jones. "$\mathcal{PT}$-symmetric sinusoidal optical lattices at the symmetry-breaking threshold". Phys. Rev. A **84**, 013818 (2011).

[22] M.-A. Miri, A. Regensburger, U. Peschel, and D. N. Christodoulides. "Optical mesh lattices with $\mathcal{PT}$ symmetry". Phys. Rev. A **86**, 023807 (2012).

[23] M. Ornigotti and A. Szameit. "Quasi $\mathcal{PT}$-symmetry in passive photonic lattices". J. Opt. **16**, 065501 (2014).

[24] T. Shui, W.-X. Yang, L. Li, and X. Wang. "Lop-sided Raman-Nath diffraction in $\mathcal{PT}$-antisymmetric atomic lattices". Opt. Lett. **44**, 2089–2092 (2019).

[25] M. Drong, M. Dems, J. Peřina Jr., T. Fordos, H. Y. Jaffres, K. Postava, and H. J. Drouhin. "Time-dependent laser cavity perturbation theory: Exploring future nano-structured photonic devices in semi-analytic way". J. Lightwave Technol. **40**, 4735—4745 (2022). url: https://opg.optica.org/jlt/abstract.cfm?URI=jlt-40-14-4735.

[26] R. El-Ganainy, K. G. Makris, D. N. Christodoulides, and Ziad H. Musslimani. "Theory of coupled optical $\mathcal{PT}$-symmetric structures". Opt. Lett. **32**, 2632–2634 (2007).

[27] H. Ramezani, T. Kottos, R. El-Ganainy, and D. N. Christodoulides. "Unidirectional nonlinear $\mathcal{PT}$-symmetric optical structures". Phys. Rev. A **82**, 043803 (2010).

[28] A. A. Zyablovsky, A. P. Vinogradov, A. A. Pukhov, A. V. Dorofeenko, and A. A. Lisyansky. "$\mathcal{PT}$-symmetry in optics". Physics-Uspekhi **57**, 1063—1082 (2014).

[29] M. Ögren, F. K. Abdullaev, and V. V. Konotop. "Solitons in a $\mathcal{PT}$-symmetric $\chi^{(2)}$ coupler". Opt. Lett. **42**, 4079–4082 (2017).

[30] J. Naikoo, K. Thapliyal, S. Banerjee, and A. Pathak. "Quantum Zeno effect and nonclassicality in a $\mathcal{PT}$-symmetric system of coupled cavities". Phys. Rev. A **99**, 023820 (2019).

[31] B. Peng, Ş. K. Özdemir, F. Lei, F. Monifi, M. Gianfreda, G. L. Long, S. Fan, F. Nori, C. Bender, and L. Yang. "Parity–time-symmetric whispering-gallery microcavities". Nat. Phys. **10**, 394–398 (2014).

[32] B. Peng, Ş. K. Özdemir, S. Rotter, H. Yilmaz, M. Liertzer, F. Monifi, C. M. Bender, F. Nori, and L. Yang. "Loss-induced suppression and revival of lasing". Science **346**, 328–332 (2014).

[33] X. Zhou and Y. D. Chong. "$\mathcal{PT}$ symmetry breaking and nonlinear optical isolation in coupled microcavities". Opt. Express **24**, 6916–6930 (2016).

[34] I. I. Arkhipov, A. Miranowicz, O. Di Stefano, R. Stassi, S. Savasta, F. Nori, and Ş. K. Özdemir. "Scully-Lamb quantum laser model for parity-time-symmetric whispering-gallery microcavities: Gain saturation effects and nonreciprocity". Phys. Rev. A **99**, 053806 (2019).

[35] I. I. Arkhipov, A. Miranowicz, F. Minganti, and F. Nori. "Quantum and semiclassical exceptional points of a linear system of coupled cavities with losses and gain within the Scully-Lamb laser theory". Phys. Rev. A **101**, 013812 (2020).

[36] F. Quijandría, U. Naether, Ş. K. Özdemir, F. Nori, and D. Zueco. "$\mathcal{PT}$-symmetric circuit QED". Phys. Rev. A **97**, 053846 (2018).

[37] A. Guo, G. J. Salamo, D. Duchesne, R. Morandotti, M. Volatier-Ravat, V. Aimez, G. A. Siviloglou, and D. N. Christodoulides. "Observation of $\mathcal{PT}$-symmetry breaking in complex optical potentials". Phys. Rev. Lett. **103**, 093902 (2009).

[38] C. Tchodimou, P. Djorwe, and S. G. Nana Engo. "Distant entanglement enhanced in $\mathcal{PT}$-symmetric optomechanics". Phys. Rev. A **96**, 033856 (2017).

[39] D.-Y. Wang, C.-H. Bai, S. Liu, S. Zhang, and H.-F. Wang. "Distinguishing photon blockade in a $\mathcal{PT}$-symmetric optomechanical system". Phys. Rev. A **99**, 043818 (2019).

[40] R. El-Ganainy, M. Khajavikhan, and L. Ge. "Exceptional points and lasing self-termination in photonic molecules". Phys. Rev. A **90**, 013802 (2014).

[41] F. Minganti, D. Huybrechts, C. Elouard, F. Nori, and I. I. Arkhipov. "Creating and controlling exceptional points of non-Hermitian Hamiltonians via homodyne Lindbladian invariance". Phys. Rev. A **106**, 042210 (2022).

[42] M. V. Berry and M. Wilkinson. "Diabolical points in the spectra of triangles". Proc. R. Soc. London A **392**, 15–43 (1984).

[43] J. Peřina Jr., A. Miranowicz, G. Chimczak, and A. Kowalewska-Kudłaszyk. "Quantum Liouvillian exceptional and diabolical points for bosonic fields with quadratic Hamiltonians: The Heisenberg-Langevin equation approach". Quantum **6**, 883 (2022).

[44] I. I. Arkhipov, A. Miranowicz, F. Minganti, Ş. K. Özdemir, and F. Nori. "Dynamically crossing diabolic points while encircling exceptional curves: A programmable symmetric-asymmetric multimode switch". Nature Commun. **14**, 2076 (2023).

[45] F. Minganti, A. Miranowicz, R. Chhajlany, and F. Nori. "Quantum exceptional points of non-Hermitian Hamiltonians and Liouvillians: The effects of quantum jumps". Phys. Rev. A **100**, 062131 (2019).

[46] F. Minganti, A. Miranowicz, R. W. Chhajlany, I. I. Arkhipov, and F. Nori. "Hybrid-Liouvillian formalism connecting exceptional points of non-Hermitian Hamiltonians and Liouvillians via postselection of quantum trajectories". Phys. Rev. A **101**, 062112 (2020).

[47] J. Peřina. "Quantum statistics of linear and nonlinear optical phenomena". Kluwer, Dordrecht. (1991).

[48] J. Peřina Jr. "On the equivalence of some projection operator techniques". Physica A **214**, 309—318 (1995).

[49] I. I. Arkhipov, F. Minganti, A. Miranowicz, and F. Nori. "Generating high-order quantum exceptional points in synthetic dimensions". Phys. Rev. A **101**, 012205 (2021).

[50] J. Peřina Jr., K. Thapliyal, G. Chimczak, A. Kowalewska-Kudłaszyk, and A. Miranowicz. "Multiple quantum exceptional, diabolical, and hybrid points in multimode bosonic systems: II. nonconventional $\mathcal{PT}$-symmetric dynamics, unidirectional coupling and general genuine points". Quantum **arxiv:**, 2405.01666 (2025).

[51] I. I. Arkhipov, A. Miranowicz, F. Nori, Ş. K. Özdemir, and F. Minganti. "Fully solvable finite simplex lattices with open boundaries in arbitrary dimensions". Phys. Rev. Res. **5**, 043092 (2023).

[52] L. Mandel and E. Wolf. "Optical coherence and quantum optics". Cambridge Univ. Press, Cambridge. (1995).

[53] A. Lukš, V. Peřinová, and J. Peřina. "Principal squeezing of vacuum fluctuations". Opt. Commun. **67**, 149—151 (1988).

[54] V. V. Dodonov. "Nonclassical states in quantum optics: A squeezed review of the first 75 years". J. Opt. B: Quantum Semiclass. Opt. **4**, R1—R33 (2002).

[55] G. Chimczak, A. Kowalewska-Kudłaszyk, E. Lange, K. Bartkiewicz, and J. Peřina Jr. "The effect of thermal photons on exceptional points in coupled resonators". Sci. Rep. **13**, 5859 (2023).

[56] R. W. Boyd. "Nonlinear optics, 2nd edition". Academic Press, New York. (2003).

[57] W. Vogel and D. G. Welsch. "Quantum optics, 3rd ed.". Wiley-VCH, Weinheim. (2006).

[58] J. Peřina Jr. and J. Peřina. "Quantum statistics of nonlinear optical couplers". In E. Wolf, editor, Progress in Optics, Vol. 41. Pages 361–419. Elsevier, Amsterdam (2000).

[59] H. Hodaei, A. U. Hassan, S. Wittek, H. Garcia-Gracia, R. El-Ganainy, D. N. Christodoulides, and M. Khajavikhan. "Enhanced sensitivity at higher-order exceptional points". Nature (London) **548**, 187–191 (2017).

[60] H. Jing, Ş. K. Özdemir, H. Lu, and F. Nori. "High-order exceptional points in optomechanics". Sci. Rep. **7**, 3386 (2017).